Middle Miocene (Serravallian) wetland development in the Kenslow Member of the Brassington Formation, central England

Jessica McCoy[a*], Tabitha Barrass-Barker[a], Emma P Hocking[a], Jennifer M O'Keefe[b], James B Riding[c], Matthew J Pound[a]

[a]Department of Geography and Environmental Sciences, Northumbria University, Newcastle upon Tyne NE1 8ST, UK

[b]Department of Physics, Earth Science, and Space Systems Engineering, Morehead State University, Morehead, Kentucky KY 40351, USA

[c]British Geological Survey, Keyworth, Nottingham NG12 5GG, UK

*Contact author: Jessica McCoy (jessica.mccoy@northumbria.ac.uk), Department of Geography and Environmental Sciences, Northumbria University, Newcastle upon Tyne, NE1 8ST, UK

Keywords: Lignite, climate change, Miocene, palynology, vegetation, UK

Abstract

The Middle Miocene was a warmer and wetter interval than present-day (Steinthorsdottir *et al*., 2021). In the UK, the most extensive Middle Miocene deposit is the Serravallian Kenslow Member of the Brassington Formation as exposed at Bees Nest Pit, near Brassington, Derbyshire, UK. While known to contain a diverse palynological and palaeobotanical record, the stratigraphical distribution of these fossils has not been studied in detail, thus biome variations through a most important proxy period are very poorly understood. This important unit has never been the subject of a detailed, multi-sample study. Here we present a 58-sample record covering 133 cm of clay and lignite. The results comprise the first reconstruction of a bog succession in the Miocene palaeobotanical record of the UK. A predominant warm-temperate and mixed mesophytic forest biome was present. Within this forest, the local wetland developed in response to environmental changes that were not related to any major climatic shift. This wetland development produced a relatively open shrub and reed-dominated mire which produced the lignite-precursor peat. The limited extent of the lignite lentil and its position adjacent to a preserved fallen tree suggests that the peat was deposited in a tree throw, although it is not possible to rule out a slightly deeper stagnant pond within the overall wetland environment.

1. Introduction

The climate of the Miocene (23.03–5.33 Ma) was warmer and wetter than present-day and has been identified as an interval of interest in the IPCC AR6 report (Pound et al., 2012a; Steinthorsdottir *et al*., 2021; IPCC, 2022). Predicted mid to late 21st century carbon dioxide (CO_2) concentrations are comparable to those reconstructed for the Middle Miocene (400–600 ppm) (Steinthorsdottir *et al*., 2021). The presence of a reduced Antarctic ice mass, less northern hemisphere ice, a recognisable palaeogeography and biota also make the Miocene a significant interval for exploring warmer than present climates and the biota that inhabited them (Pound *et al*., 2011). Global climates cooled during the Middle Miocene Climate Transition (MMCT: 14.5–12.5 Ma) in a step-like manner, but remained warmer than present day (Quaijtaal *et al*., 2014; Steinthorsdottir *et al*., 2021). During this interval, sea surface temperature gradients between 42 °N and 57 °N in the North Atlantic collapsed and remained so until around 7.6 Ma; these flat sea surface temperature gradients were interpreted to be a precursor to the modern North Atlantic Current and kept the mid-latitude North Atlantic relatively warm during the MMCT (Super *et al*., 2020). Palaeobotanical evidence from the North Atlantic region also points to formation of the North Atlantic Current during the Middle Miocene (Denk *et al*., 2013; Pound and Riding, 2016; Pound and McCoy, 2021).

Across northwest and Central Europe, this interval was characterised by relatively stable mean annual precipitation with extensive wetland environments (van Dam, 2006; Utescher *et al*., 2021).

The British Isles archipelago formed a northwest-trending peninsula on the European continent during the MMCT (Steinthorsdottir *et al*., 2021). Unfortunately, onshore terrestrial Miocene sediments are not common in this region (Gibson *et al*., 2022). Of the three known fossiliferous sites, the St. Agnes Outlier in Cornwall has considerable dating uncertainty (Walsh *et al*., 1987) and Trwyn y Parc in Anglesey is Langhian, probably pre-MMCT (Pound and McCoy, 2021; Gibson *et al*., 2022). This only leaves the diachronous Kenslow Member of the Brassington Formation (Serravallian–Tortonian) as a possible comparable environment to those observed in northwest and central Europe (Ivanov *et al.*, 2007a-b; Jiménez-Moreno *et al*., 2008; Hui *et al*., 2011; Larsson *et al*., 2011; Szulc and Worobiec, 2012; Pound *et al.*, 2012b; Velitzelos *et al*., 2014; Pound and Riding, 2016; Utescher *et al*., 2017). Previous research on the Kenslow Member at the Kenslow Top Pit has shown a relatively stable palynoflora dated as early Tortonian (Boulter, 1971a-b), although only productive grab samples have been analysed from the Serravallian and late Tortonian Kenslow Member outcrops at the Kenslow Top Pit and Bees' Nest Pit, see Figure 1 for locations (Pound *et al*., 2012b; Pound and Riding, 2016).

This study is the first to report a continuous palynological record from the Serravallian portion of the Kenslow Member and provides a unique insight into the terrestrial environments present on an Atlantic peninsula prior to full formation and stabilisation of the North Atlantic Current (Super *et al*., 2020).

1.2. The geology of the Kenslow Member

The Kenslow Member is the uppermost of three members that form the Brassington Formation of Derbyshire and Staffordshire in central England (Figures 1-2). Preserved in around 60 karstic hollows, the Brassington Formation is dominated by the unfossiliferous Kirkham and Bees Nest members, whilst the fossiliferous Kenslow Member has only been identified at seven locations (Boulter *et al*., 1971; Boulter, 1971b; Walsh *et al*., 2018). The Kirkham Member comprises up to 70 m of palaeontologically-barren cream/white and red/brown sands intercalated with pebble layers, and which represent the erosional products from the Triassic sandstone escarpment to the south of Brassington according to Yorke (1954), Boulter *et al*. (1971), and Walsh *et al*. (1980; 2018). The Bees Nest Member is around 6 m of varicoloured unfossiliferous clays and silts (Boulter *et al*., 1971; Ford and Jones, 2007; Walsh *et al*., 2018). The uppermost Kenslow Member contains plant-bearing grey clays and lignite (Boulter *et al*., 1971; Walsh *et al*., 1972; Walsh *et al*., 1980; O'Keefe *et al*., 2020). The Kenslow Member is diachronous on pollen evidence (Pound and Riding, 2016). At Bees Nest Pit,

near Brassington village, Derbyshire, UK (Figure 1) this unit is Serravallian, whereas at the Kenslow Top Pit, near Friden, it is of Tortonian in age (Pound *et al*., 2012b; Pound and Riding, 2016). Both these disused quarries have previously yielded a wide range of palaeobotanical remains, including Cupressaceae seeds, fungal remains, leaves, pollen grains, spores and wood (Boulter and Chaloner, 1970; Boulter, 1970; Boulter *et al*., 1971; Boulter, 1974; Pound *et al*., 2012b; Pound and Riding, 2016; Pound *et al*., 2019; O'Keefe *et al*., 2020; Table 1).

Figure 1

The Brassington Formation is thought to have formed in an alluvial-fluvial-lacustrine depositional setting before being incorporated into its present-day karstic setting (Boulter *et al*., 1971; Walsh *et al*., 1972; 1980; 2018). Bees Nest Pit and Kenslow Top Pit exhibit structures interpreted to be subsidence-related sag synclines and recent developments in the understanding of hypogene processes suggest post-Miocene uplift triggered suffusion processes (Walsh *et al*., 1972; 1980; 2018). The setting of the organic-rich Kenslow Member has been proposed to be an isolated lake (Walsh *et al*., 2018) or a sinkhole pond (Pound *et al*., 2012b).

1.3. Previous palynological investigations of the Kenslow Member

Previous studies have identified a diverse assemblage of more than 60 pollen and spore taxa from the Kenslow Member at Bees Nest and Kenslow Top pits (Boulter and Chaloner, 1970; Boulter, 1971a-b; Pound *et al*., 2012b; Pound and Riding, 2016). Boulter (1971a) presented a succession of samples from Kenslow Top Pit that showed a relatively stable pollen and spore assemblage dominated by Ericaceae (<37%), triporates (<30%) and *Tricolpopollenites liblarensis* (<17%). A single sample was also presented from Bees Nest Pit that was dominated by relative abundances of *Pinus* haploxylon-type (<20%), *Quercoidites microhenrici* (10%) and *Sciadopitys* (8%). Pound *et al*. (2012b) located an unstudied section of the Kenslow Member at Kenslow Top Pit, which contained a single productive sample that differed from the previous assemblage found by Boulter (1971a). This was dominated by *Compositoipollenites rhizophorus* (20%), *Stereisporites* (12%), *Pinus* (10%), Ericaceae (8%) and *Trivestibulopollenites betuloides* (4%) and led Pound *et al.* (2012b) to assign a late Tortonian (younger than 9 Ma) date to the entire Kenslow Member. The rediscovery of a Kenslow Member section at Bees Nest Pit (Figure 1) and fossil wood stored in the British Geological Survey archives, led Pound and Riding (2016) to propose diachronous dates for different Kenslow Member outcrops. The original Kenslow Top Pit of the Kenslow Member outcrop is no longer visible in the field, but wood recovered by Yorke (1960) contained Kenslow Member clay filled cracks. This yielded

an assemblage comparable to Boulter (1971a) dominated by Ericaceae pollen types and, notably, *Triplanosporites sinuosus* (Pound and Riding, 2016). The Kenslow Member sample from Bees Nest Pit was found to be dominated by conifer pollen, especially *Cathaya*, *Pinus*, *Sciadopitys* and *Tsuga* (Pound and Riding, 2016). Angiosperms were present, but only *Carya,* Ericaceae and *Ilex* formed significant proportions of the assemblage (Pound and Riding, 2016). Combined with the sample presented in Pound et al. (2012b), it was determined that the palynoflora from the Kenslow Member at Bees Nest Pit is comparable to the younger Serravallian of the Lower Rhine Basin, whilst the two samples from Kenslow Top Pit are more comparable to the Dutch and German Tortonian (Pound and Riding, 2016). Climatically, this sequence of samples from the different outcrops of the Kenslow Member showed decreasing temperatures, precipitation and seasonality from the late Serravallian to the late Tortonian (Pound et al., 2012b; Pound and Riding, 2016; Gibson et al., 2022). The Kenslow Member at Bees Nest Pit has only ever been studied from grab samples. This presents a major omission in our knowledge of the palaeoenvironments and palaeoclimates of northwest Europe during an interval of abnormal North Atlantic temperature gradients (Super *et al*., 2020). In this paper we present the first sequence of 58 palynological samples taken through the lignite and clay from the Serravallian Kenslow Member at Bees Nest Pit. These are used to reconstruct the palaeoenvironment and palaeoclimate during the later Serravallian.

2. Materials and methods

A clay and lignite column, measuring 133 cm-thick, was extracted from the type section of the Kenslow Member at Bees Nest Pit at 53˚05'16.9"N, 1˚38'28.6"W (Figure 2). Fifty-eight samples, weighing 1–2 g were taken using a sterilised spatula at 1 cm-intervals from the lignite section (5–21 cm), and from 1–5 cm-intervals throughout the clay (22–133 cm). Twenty-five samples were taken for grain size analysis using the Mastersizer 2000 at 3–5 cm intervals. A non-acid technique was used following Riding and Kyffin-Hughes (2006) that involved disaggregating samples in hot water and sieving through 125 µm and 10 um nylon mesh sieves (Pound *et al*., 2021; Riding, 2021). Sieved residues were centrifuged at 3300 rpm for 3 minutes to remove excess water. Copper sulphate was added to samples to prevent microbial growth. Permanent slides were produced using 0.1 ml of Kaiser's glycerol jelly. Where high silica content obscured the view of palynomorphs (22–133 cm), samples were swirled on a watch glass to separate the quartz grains from the palynomorphs (Pound *et al*., 2021; Riding, 2021). Pollen and spores were identified and counted using a Leica DM500 light microscope at x400 magnification. The pollen and spore descriptions of Boulter (1971a) and Stuchlik *et al*. (2001; 2002; 2009; 2014) were used for taxonomical identifications.. Nearest living relatives of

154 fossil taxa were determined by botanical affinities listed Stuchlik *et al*. (2001; 2002; 2009; 2014).
155 Photomicrographs were obtained using an integral ICC50W digital camera operated by Leica
156 Application Suite® software (Figure 3).

157 **Figure 2**

158 For each sample, the Shannon Index was calculated to assess the pollen diversity throughout
159 the Kenslow Member (Shannon and Weaver, 1949). *Juglans*, *Nyssa* and *Symplocos* pollen-types were
160 quantified to show the proportion of Cool-Tolerant extinct European taxa of East Asian affinity (CTEA)
161 (Martinetto *et al*., 2017). The relative abundance of CTEA-assigned taxa was summed at each depth.
162 The co-existence approach was used to reconstruct the Mean Annual Temperature (MAT), Mean
163 Annual Precipitation (MAP), Coldest Month Mean Temperature (CMMT) and Warmest Month Mean
164 Temperature (WMMT) (Utescher *et al*., 2014). The co-existence approach is a nearest living relative
165 technique, where each fossil taxon is assigned its nearest living relative, and the modern climate
166 tolerances of the nearest living relatives are used to reconstruct the fossil climate (Mosbrugger and
167 Utescher, 1997; Utescher *et al*., 2014). Relict taxa i.e. *Cathaya*, *Cercidiphyllum* and *Sciadopitys* were
168 removed as their present-day biogeography is limited, and their Neogene niches covered a larger
169 range of palaeoenvironments (Mosbrugger *et al*., 1994; Figueiral *et al*., 1999). Nearest living relatives
170 were assigned to taxa using Stuchlik *et al*. (2001; 2002; 2009; 2014).

171

172 ## 3. Results

173 ### 3.1. Grain size analysis and interpretation

174 The Kenslow Member at Bees Nest Pit comprises 112 cm of grey, silty clay, containing small
175 and large fragments of fossil wood, with a 21 cm-thick lignite lentil at the top (Figures 2, 4-5). Grain
176 size analysis shows little change until 15 cm, when sand-sized particles of fossil plant remain within
177 the lignite increase at the expense of clay. This coarsening-upwards trend does not, therefore,
178 indicate an increase in energy of the drainage channels supplying this lacustrine environment as
179 would be the case if there had been an influx of sand. By contrast, the presence of the lentil of
180 lignite at the top of this clay succession probably indicates shallowing, and the development of a
181 wetland.

182 ### 3.2. Palynology: Zone KM19-1 (57-133 cm)

183 Descriptions of relative abundances in Sections 3.2 and 3.3 refer to Figure 4-5. Informal
184 pollen Zone KM19-1 contains an assemblage of Cupressaceae (3-16%); *Tsuga* (34-8%);

Tricolpopollenites liblarensis (10-3%); *Quercoidites microhenrici* (1-7%); *Sciadopitys* (1-11%) and Cyrillaceae/ Clethraceae (0-4%). *Tsuga*-type achieves its highest values between 120–105 cm (34-27%), whilst *Betula* (10%) peaks at 125 cm. *Betula*-type then decreases from the remainder of the zone. Following peak *Tsuga* abundance, Cyrillaceae (<7%), *Olea*-type (<6%), *Salix*-type (<3%) and *Tricolpopollenites ipilensis* (5%) all peak in this zone between 105 and 80 cm. Following this interval, these taxa decrease in relative abundance or become near-absent for the remainder of the zone. Between 105 and 75 cm, Cyperaceae, *Sphagnum,* and *Typha*-type all disappear from pollen zone KM19-1. In contrast, *Abies* and *Pinus*-type. begin to increase in relative abundance between 80–75 cm. Pollen diversity declines from 85 cm to its lowest level for the entire record. KM19-1 shows increasing relative abundance of riparian elements become most sporadic in the woody lignite section (Figure 4). Until 69–61 cm, *Betula*-type decreases, then begins to increase again, peaking at the end of this zone. Cupressaceae and *Sciadopitys* achieve their highest relative abundances (14% and 15%, respectively).

3.3. Palynology: Zone KM19-2 (5-57 cm)

Informal Zone KM19-2 contains an assemblage of *Pinus* (<15%); *Tricolpopollenites liblarensis* (<10%), *Castaneioideae* (8%), Cupressaceae (<18%) and *Betula*-type (19%). At 55 cm, *Pinus* (15%) and *Abies* (10%), *Picea* (5%) and *Cathaya* (4%) relative abundances peak alongside *Tsuga* (14%). Relative abundances of Compositae and *Cercidiphyllum* peak between 42–45 cm at 4% and are then near-absent throughout Zone KM19-2 alongside *Abies*, which peaks between 37–43 cm (11%). Figure 4 shows from 35 cm, *Sphagnum* is once again present from 38 cm, having been absent since 75 cm. Relative abundances of *Tsuga* and *Sciadopitys* peak at 33 cm (21% and 13%, respectively), with *Pinus* (12%), *Tricolpopollenites fallax* (8%), *T. liblarensis* (7%) and Castaneioideae (4%), demonstrating increasing, following relative abundances at 32 cm, alongside a reduction in the Shannon index. From 24–29 cm relative abundances of *Alnus* (<7%), Ericaceae (<6%) and *Cedrus* (<6%) increase. *Quercus* peaks at 27 cm (7%) alongside *Juglans*, which reaches a zonal peak from 25–27 cm (3%). Throughout the lignite section (5–21 cm), relative abundances of *Alnus* (<7%), *Betula* (<19%) and *Cedrus* (<4%) increase towards the surface. At 15 cm, peaks of relative abundances of *Picea* (16%) and *Pinus* (16%) occur. The increase in CTEA at 15 cm is driven by a peak in *Symplocos* (11%), and a decrease in the Shannon index value strongly suggests a low diversity zone (Figure 4). Poaceae peaks at 14 cm (8%). *Nyssa* emerges in higher depths, peaking at 7 cm (2%). *Tricolpopollenites ipilensis,* Fabaceae-types (*T. liblarensis* and *T. fallax*) increase alongside increased numbers in the Shannon and CTEA indexes. *Tsuga* peaks in the final sample (5 cm, 15%) whereas Cupressaceae declines towards 5 cm. Relative abundance of CTEA reaches its lowest level for the entire record at 8 cm (Figure 4). Figure 4 shows relative abundances of Cyperaceae (<5%), *Sphagnum* (<4%) and *Typha*-

types (<2%) increase towards the top of this succession. Zone KM19-2 shows increased diversity of relative abundances of taxa. KM19-2 shows increased relative abundance of angiosperms and mixed forest taxa. Relative abundance of riparian swamp elements become most sporadic in the woody lignite section (Figures 4-5).

Figures 4-5

3.4. Palaeoclimate reconstruction

Reconstructed palaeoclimate ranges refer to those presented on Figure 6 and in Supplementary Table 2; delimiting taxa are listed below. The co-existence approach reconstructed relatively consistent and unchanging MAT, MAP, CMMT and WMMT values. The co-existence approach reconstructs a MAT of 15.7–18.4 °C (widest reconstruction being 15.6–21.7 °C). Presence of *Picea*-types influenced the widest reconstructions of MAT (21.7 ˚C). Modal MAT reconstructions were delimited by *Keteleeria* and *Cedrus*. *Keteleeria* delimited modal MAP (1096 mm) reconstructions, respectively. The reconstructed CMMT was 5.0–12.5 °C (widest reconstruction being 1.8–12.5 °C), and the reconstructed WMMT was 24.7–27.9 °C (widest reconstruction being 23.6–28.3 °C). Uppermost widest WMMT reconstructions were controlled by *Quercus* relative abundance. Relative abundances of *Compositae*-types delimited the widest reconstructions of MAT (15.7 ˚C) and the lowermost modal CMMT and WMMT reconstructions (5 ˚C and 24.7 ˚C, respectively). Uppermost modal WMMT reconstructions considered *Nyssa* relative abundance (27.9 ˚C). Presence of *Symplocos*-types delimited the lower bound of the widest CMMT (1.8 ˚C) and WMMT (23.6 ˚C) reconstructions. *Cedrus*-types influenced upper modal MAT reconstructions (18.4 ˚C) and the lowest widest WMMT reconstructions (12.5 ˚C). The reconstructed MAP range was 1096–1372 mm (widest reconstruction being 703–1682 mm). MAP reconstructions were delimited by *Lygodium* (703 mm), *Olea* (1372 mm) and *Corylus* (1682 mm).

Figure 6

4. Discussion

The palynology of the Kenslow Member at Bees Nest Pit overall indicates a mixed mesophytic forest and a small evolving wetland environment within a wider forested landscape (Figure 7). Reconstructed temperatures point to a warm-temperature to subtropical climate with relatively high MAP that are comparable to previously published reconstructions (Figures 6, 8; Pound and Riding, 2016; Gibson *et al*., 2022).

Figure 7

Compared to other Serravallian co-existence approach-based MAT reconstruction from Europe, those bordering the North Atlantic are warmer (Figure 8). This likely shows the influence of a proto-North Atlantic Current (Super et al., 2020). There is no evidence for substantial climate change in the section based upon the overlapping ranges of all reconstructed palaeoclimate ranges (Figure 6). This provides additional evidence to support an environmental, rather than climatic, control on the changing pollen and spore assemblages throughout the KM19 section. However, the relatively wide ranges reconstructed for MAP and CMMT do not preclude modest changes having occurred within these variables (Figure 6); frost-free winters occurred, like ?Langhian European reconstructions (Pound and McCoy, 2021). Despite the consistent nature of the climate reconstructions, there are a number of changes in the pollen and spore sequence from the KM19 section (Figures 4-5). Within the assemblage are elements of a *Pinus*-bog transitioning to an umbrella pine wetland with mixed mesophytic forest elements (Schneider, 1992; Figure 7). Bush and reed-marsh mire facies elements (e.g.: *Tricolpopollenites liblarensis* and *T. fallax*) are present, indicative of a more open canopy mire environment (Schneider, 1992; Figure 4; 7). The assemblages show similarities with other Miocene palaeoenvironment reconstructions in Central Europe, except for *Tsuga*-types which are typically present in only minor quantities in these assemblages – not dominant, as in KM19 (Schneider, 1995; Figueiral *et al*., 1999; Ivanov *et al*., 2007a; Larsson *et al*., 2011; Kern *et al*., 2012). Similar present-day assemblages exist west of the Cumberland Mountains and the Appalachian Mountains, Kentucky, North America in the Daniel Boone forest (Parker, 1985), which are dominated primarily by *Nyssa*, *Quercus* and Fagaceae, which reflect a warm-temperate mixed forests (Braun, 1942; Box, 2015). High relative abundances of coniferales (*Sciadopitys*, Cupressaceae, *Tsuga*-types) are common in Holocene-age and present-day assemblages from East Asia (Uemura, 1986; Igarashi *et al*., 2018).

Figure 8

Tsuga pollen dominates the assemblage, reaching 34% relative abundance at 120 cm (Figures 4-5; Figure 7: Stages A-B). Extant species of *Tsuga* require high humidity and are not tolerant of drought or fire (Thompson *et al*., 1999; Fusco, 2010). High relative abundances of *Tsuga* pollen are not common in European Miocene assemblages (Figueiral *et al.*, 1999; Pound *et al*., 2012b; Pound and Riding, 2016). Maximum amounts of 10% were previously reported for the Kenslow Member (Pound and Riding, 2016). High relative abundance of *Tsuga*-types with *Sciadopitys*-types occurs in coniferous forest assemblages of the uppermost Miocene–Pliocene Poznań Clays of Poland (Piwocki and Ziembińska-Tworzydło, 1997; Figure 4). Although *Pinus* pollen is not present until nearly the end

of pollen zone KM19-1, high relative abundance of *Pinus* pollen in the Poznań Clays is coeval with high *Tsuga* and *Sciadopitys* counts (Piwocki and Ziembińska-Tworzydło, 1997, Figure 4). In the Poznań Clays, this is coeval with high *Pinus*-type pollen, while at Bees Nest, *Pinus*-type pollen is not present until nearly the end of the pollen zone KM19-1, when the reconstruction of a pine-dominant bog type is present (Figure 7).

Following peak abundance of *Tsuga* pollen, at 105 cm, there is an interval of wetlanddevelopment (Figure 7: Stage B). This assemblage is characterised by wet-tolerant *Salix, Sciadopitys*, *Nyssa* and *Myrica*-types which together are suggestive of margin or perhaps domed conditions (Dai *et al*., 2020). Conditions are like those in ombrotrophic peatlands formed in Amazonian floodplains and East Asian peatlands, which are sustained by high precipitation rates and mycorrhizal fungal-floral relationships (Lähteenoja *et al.*, 2009; Page *et al*., 2010; Dai *et al*., 2020). The occurrence of the shrub *Itea*-type (from 53 cm) is also suggestive of a small understory within the wetland environments, proximal to the depositional basin, as the shrub's modern preferred habitats range from wetlands to stream and lake margins (Figure 4; Ivanov *et al*., 2007a).

Cyrillaceae/ Clethraceae, Ericaceae, *Myrica* and *Ilex* relative abundances are highest and most consistent in KM19-1, compared to their respective relative abundances in KM19-2 (Figures 4-5) and are resemblant of assemblages found within modern mires found from Virginia to northern Florida, USA (Richardson, 2003; Worobiec *et al*., 2021). Assuming comparability with North American present-day assemblages, *Myrica*-types will have affinity to *Morella caroliniensis* (Wilbur, 1994; 2002). Pollen Zone KM19-1 is entirely in the clay layer with large fragments of wood, and alternates between silty-clay and clayey-silt grain sizes (Figure 4; Figure 7: Stages A-C). In sedimentological terms, this could be indicative of a floodplain setting, given the implied decrease in fluvial transport capacity associated with plant fragments and lignite, as described by Joniak *et al*. (2020). The pollen assemblages show that the hinterland of the lake was covered by a conifer-dominated mixed forest (Schneider, 1992; Figure 7: Stages A-B). Although not yet fully studied, the fossil wood shows extensive evidence for fungal decay and subaerial cracking (O'Keefe *et al*., 2020). Previous fungal remains, extracted from a sediment-filled crack in one fossil wood specimen, contain saprobic taxa that required submerged environments (Pound *et al*., 2019). This provides some additional evidence for an environment where previously exposed dead wood became incorporated into the peat. The development of a more open canopy wetland could be due to development of a gap in the conifer dominated mixed forest, often resultant of fire regimes (Gates, 1942; Schwintzer, 1981), though without reported charcoal abundance, claims are merely suggestive (Rius *et al.*, 2011; Wolf *et al*., 2013). A slow-rising water table resulting from wet periods may also be responsible for drowning of wet-intolerant shallow-rooted flora, which lead to increased wetland productivity (Schwintzer, 1981;

Preston, 1996). This could have been achieved through individual treefalls, as suggested by Wilde and Riegel (2021), or through periodic fire (Ravazzi *et al*., 2005; Fusco, 2010).

Mixed mesophytic forest taxa initially dominated KM19-2 at 57 cm (75%), most influenced by coniferous pollen relative abundance, that implies the establishment of a *Pinus*-bog and then, potentially, a *Sciadopitys* raised bog at 33 cm (Schneider, 1992; Figures 4-5). Extant Castaneioideae species can grow quickly to exploit the canopy opening prior to the establishment of other trees (Frothington, 1912; Nichols, 1913; Foster and Zebryk, 1993). Cupressaceae wetland development occurs most prominently from 29 cm (30%) (Figure 4; Figure 7: Stage C), with corresponding high relative abundances of *Alnus* (7%) and *Betula*-types (9%) around the swamp margin (Schneider, 1992; Larsson *et al*., 2011; Akyurt *et al*., 2016; Worobiec *et al*., 2021; Figure 4). *Alnus* and *Betula* peak with increased autochthonous herbaceous pollen which lined the wetland edge as is also seen in Middle Miocene assemblages from the Adamów lignite deposit (Worobiec *et al*., 2021).

Increased relative abundance in Cyperaceae, *Sphagnum*-type and *Typha*-type, from 50 cm, are suggestive of developing wetland environments (Doren *et* al., 1997; Kern *et al.*, 2012; Figure 4). Extant *Nyssa*-types obligate to facultive members of wetland biomes in the present-day United States if interspecific competition from shrubs and herbs is limited. Relative abundances of warm-temperate taxa such as Compositae and *Cercidiphyllum*-type establish (45-43 cm), then decline (33 cm) to near-absent (Figure 4; Figure 7: Stage D). Extant *Cercidiphyllum* colonises a variety of open floodplain environments, and its sporadic relative abundance throughout KM19-2 may suggest intermittent establishment on a floodplain (Crane, 2008; Wei *et al*., 2010; Figure 4; Figure 7: Stage D). Fabaceae-types likely come from plants of both the shrub layer and the undergrowth, and has a clear affinity with previous swamp phases, given its gradual decrease in relative abundance at 39–32 cm after the development towards an umbrella pine wetland with mixed mesophytic forest elements (Szulc and Worobiec, 2012, Figure 4; Figure 7: Stage D).

The limited extent of the lignite layer could mean that it represents a forest hollow created by a fallen tree, or partial subsidence of the underlying karst (Schaetzl *et al*., 1988; Pound *et al*., 2012b; Wilde and Riegel, 2021). Pioneer and lake margin taxa Cyperaceae, *Sphagnum*-type and *Typha*-type relative abundance increases in KM19-2 due to colonisation of this small wet opening (Verb and Rubino, 2012; Wilde and Riegel, 2021). Increase in *Typha*-type relative abundance suggests a stagnant environment, resulting in increased organic matter deposition (Kvaček, 2004; Hofmann and Zetter, 2005; Szulc and Worobiec, 2012). Biomass accumulated, leading to the deposition of a modest lignite lentil, defined by O'Keefe *et al*. (2013), in the upper Kenslow Member, which reconstructed a small open wetland (Figures 4-5; Figure 7: Stages D-E). *Tsuga*-type,

Sciadopitys-type, *Pinus*-type, *Tricolpopollenites fallax, T. liblarensis*, Castaneioideae relative abundance increases with decreased Shannon Index values, suggesting stabilised bog development between *Pinus*-bog and *Sciadopitys* raised-bog biomes from 16 cm (Schneider, 1992, Figure 4).

By providing a new palaeobotanical record for the Middle Miocene-age sediment of the Kenslow Member, we demonstrate that Middle Miocene UK assemblages were wetter than previously anticipated despite reconstructions of open grasslands and arid conditions from Middle Miocene assemblages from the Madrid Basin (Prista *et al*., 2015; Casas-Gallego *et al*., 2021). Our high-precipitation palaeoclimate reconstructions were likely resultant of the developing North Atlantic Current (Jiménez-Moreno *et al*., 2008; Super *et al*., 2020). Limited seasonality, given mild CMMT reconstructions of <12.5 °C show similarities to other poorly seasonal reconstructions of Burdigalian-Langhian reconstructions across Eurasia, suggesting a possible lag in seasonality increase for higher Eurasian latitudes after the Middle Miocene Climatic Optimum (Bruch *et al*., 2011; Utescher *et al*., 2015; 2017). This period of low seasonality at mid-high Eurasian latitudes has been attributed to the likely and temporary existence of a Palaeo-Gulf Stream throughout the Middle Miocene, which also was a likely contributor to near subtropical winter ?Langhian palaeoenvironments for the northwest edge of Europe (Pound and McCoy, 2021). The northwest edge of Europe shows limited step-wise cooling that is otherwise demonstrated by other palaeoclimate reconstructions across Europe (Denk *et al*., 2013). Whilst it is possible that the influence of a Palaeo-Gulf Stream would dissipate circa 15 Ma, after the closure of the Central American Seaway, we attribute maintained warming to the development of the North Atlantic Current and latent and sensible heat fluxes associated with canopy cover in Miocene forest biomes (Micheels *et al*., 2007; 2011; Bacon *et al.*, 2013; Montes *et* al., 2015; Utescher *et al*., 2015; 2017).

Comparison with other Miocene palaeoenvironmental reconstructions suggests an overall very inconsistent temperature gradient across central Europe, whereas high precipitation on the northwest edge of Europe remains more spatially consistent (Figure 8). Post-Aquitanian longitudinal temperature gradients from East and West European palaeoclimate reconstructions increased throughout the Neogene, with pronounced cooling concentrated to the East, although lowest MAT reconstructions are present within Central Europe, although the main driver of this variation is influenced by the movement of the Eurasian plate, and thus biomes in northwest Europe are unaffected (Bruch *et al*., 2011; Popova *et al*., 2012; Utescher *et al*., 2015; Figure 8). We highlight that the formation of the North Atlantic Current on the Atlantic peninsula likely contributed towards the stability of regional precipitation patterns on the northwest edge of Europe (Denk et al., 2013; Super et al., 2020). The influence of the North Atlantic Current on precipitation likely continued throughout

383 the Serravallian towards the Tortonian given high precipitation reconstructions which exceeded
384 coeval Eastern European reconstructions (Bruch *et al*., 2007; 2011).

385 We highlight that possible latitudinal shift in climate, expected resultant of 21st century
386 climate change, may cause possible increases in temperature and precipitation – although this is not
387 certain, given the complexity of climate mechanisms. Should increases in temperature and
388 precipitation be observed, climatological and vegetational dynamics on the northwest edge of
389 Europe may mimic those observed in present-day North America, particularly where the mid-
390 Appalachian Mountain range is situated, alongside trends observed in modern southeast Asia
391 (Uemura, 1986; Balcombe *et al*., 2005; Igarashi *et al*., 2018).

392

393 ## 5. Conclusions

394 From the first continuous, high-resolution pollen-spore record of the type section of the
395 Kenslow Member of the Brassington Formation at Bees Nest Pit, we report the first Miocene bog
396 succession in the UK Neogene vegetational record. A mixed mesophytic forest with a wetland that
397 contained a small bog developed in a warm-temperate to subtropical environment with relatively
398 high rainfall. The bog was dominated by elements of both *Pinus*-bog and *Sciadopitys*-raised bog
399 biomes. The two pollen zones (KM19-1 and KM19-2) indicate a transition from a *Tsuga*-dominated
400 mixed forest to a highly-diverse shrub and tree dominated forested wetland. Increased diversity
401 through the record resulted from the opening of the canopies that may have resulted from localised
402 treefall, karst subsidence or floodplain dynamics. High precipitation, compared to Central Europe, on
403 the northwest edge of Europe and frost-free conditions were likely driven by input from the proto-
404 North Atlantic Current.

405

406 ## Acknowledgements

407 The fieldwork was made possible with an Elspeth Matthews Fund granted by the Geological
408 Society to Matthew Pound in 2019. Matthew Pound thanks NERC (NE/V01501X/1) and Jennifer M.K.
409 O'Keefe thanks NSF (award #2015813) for funding ongoing research into the Middle Miocene
410 through the Fungi in a Warmer World (FiaWW) project. We are grateful to Jayne Spencer, the owner
411 of Bees Nest Pit and Natural England for facilitating access to this disused quarry. Lesley Dunlop,
412 Peter Jones, Michael Lim and Cameron Reaveley are thanked for their help with the fieldwork. Dave
413 Thomas of Northumbria University is thanked for his assistance with the Mastersizer. James B. Riding
414 publishes with the approval of the Director, British Geological Survey (NERC). The authors thank

Torsten Utescher and an anonymous reviewer for their comments which provided very helpful insight for manuscript development.

Declaration of interest

The authors report no conflict of interest.

Data Availability

Datasets related to this article (Figure 8) can be found at DOI: 10.5281/zenodo.6817464, titled "Serravallian terrestrial climate data for Europe" hosted on Zenodo (Pound, 2022).

References

Akyurt, E., Grímsson, F., Zetter, R., Leng, Q. and Bouchal, J.M. (2016) Reinvestigation of the Miocene palynoflora from the Daotaiqiao Formation of north-eastern China using SEM. In *EGU General Assembly Conference Abstracts*: EPSC2016-5601.

Bacon, C.D., Mora, A., Wagner, W.L. and Jaramillo, C.A. (2013) Testing geological models of evolution of the Isthmus of Panama in a phylogenetic framework. *Botanical Journal of the Linnean Society*, **171**(1): 287-300.

Balcombe, C.K., Anderson, J.T., Fortney, R.H., Rentch, J.S., Grafton, W.N. and Kordek, W.S. (2005) A comparison of plant communities in mitigation and reference wetlands in the mid-Appalachians. Wetlands, **25**(1): 130-142.

Boulter, M.C. (1970) *Cryptomeria* – a significant component of the European Tertiary, *Palaeobotanik B*: 279-287.

Boulter, M.C. (1971a) A palynological study of two of the Neogene plant beds in Derbyshire, *Bulletin of the British Museum (Natural History),* London, **19**(7): 1-409.

Boulter, M.C. (1971b) A survey of the Neogene flora from two Derbyshire pocket deposits, *The Mercian Geologist*, **4**(1): 45-61.

Boulter, M.C. (1974) An enigmatic fossil moss from the British Tertiary. *Journal of Bryology*, **8**(1): 65-68.

443 Boulter, M.C. and Chaloner, W.G. (1970) Neogene fossil plants from Derbyshire (England). *Review of*
444 *Palaeobotany and Palynology*, **10**(1): 61-78.

445 Boulter, M.C., Ford, T.D., Ijtaba, M. and Walsh, P.T. (1971) Brassington Formation: a newly recognized
446 Tertiary Formation in the southern Pennines. *Nature Physical Science*, **231**(23): 134-136.

447 Box, E.O. (2015) Warm-temperate deciduous forests of Eastern North America. *In* Warm-Temperate
448 Deciduous Forests around the Northern Hemisphere, Springer, Cham: 225-255.

449 Braun, E.L. (1942) Forests of the Cumberland Mountains. Ecological Monographs, **12**(4): 413-447.

450 Bruch, A.A., Uhl, D. and Mosbrugger, V. (2007) Miocene climate in Europe—patterns and evolution:
451 a first synthesis of NECLIME. *Palaeogeography, Palaeoclimatology, Palaeoecology*, **253**(1-2): 1-7.

452 Bruch, A.A., Utescher, T. and Mosbrugger, V. (2011) Precipitation patterns in the Miocene of Central
453 Europe and the development of continentality. *Palaeogeography, Palaeoclimatology,*
454 *Palaeoecology*, **304**(3-4): 202-211.

455 Casas-Gallego, M., Postigo-Mijarra, J.M., Rivas-Carballo, M.R., Valle-Hernández, M.F., Morín-de
456 Pablos, J. and Barrón, E. (2021) Early evidence of continental aridity and open-habitat grasslands in
457 Europe as revealed by the Middle Miocene microflora of the Madrid Basin. *Palaeogeography,*
458 *Palaeoclimatology, Palaeoecology*, **581**: 110603.

459 Crane, D. (2008) *Effects of Land Cover on Aquatic Communities and Food Webs: A Study of Second*
460 *Order Streams in Southeastern Michigan* (Doctoral dissertation): 1-45.

461 Dai, S., Bechtel, A., Eble, C.F., Flores, R.M., French, D., Graham, I.T., Hood, M.M., Hower, J.C., Korasidis,
462 V.A., Moore, T.A. and Püttmann, W. (2020) Recognition of peat depositional environments in coal: A
463 review. International Journal of Coal Geology, **219**: 103383.

464 Denk, T., Grimm, G.W., Grímsson, F. and Zetter, R. (2013) Evidence from"" Köppen signatures"" of
465 fossil plant assemblages for effective heat transport of Gulf Stream to subarctic North Atlantic during
466 Miocene cooling. *Biogeosciences*, **10**(12): 7927-7942.

467 Denk, T., Grimm, G.W., Grímsson, F. and Zetter, R. (2013) Evidence from" Köppen signatures" of
468 fossil plant assemblages for effective heat transport of Gulf Stream to subarctic North Atlantic during
469 Miocene cooling. *Biogeosciences*, **10**(12): 7927-7942.

470 Doren, R.F., Armentano, T.V., Whiteaker, L.D. and Jones, R.D. (1997) Marsh vegetation patterns and
471 soil phosphorus gradients in the Everglades ecosystem. *Aquatic Botany*, **56**(2): 145-163.

Figueiral, I., Mosbrugger, V., Rowe, N.P., Ashraf, A.R., Utescher, T. and Jones, T.P. (1999) The Miocene peat-forming vegetation of northwestern Germany: an analysis of wood remains and comparison with previous palynological interpretations. *Review of Palaeobotany and Palynology*, **104**(3-4): 239-266.

Ford, T.D. and Jones, J.A. (2007) *The geological setting of the mineral deposits at Brassington and Carsington, Derbyshire*. Peak District Mines Historical Society, **16**(5): 1-23.

Foster, D.R. and Zebryk, T.M. (1993) Long-term vegetation dynamics and disturbance history of a *Tsuga*-dominated forest in New England. *Ecology*, **74**(4): 982-998.

Frothington, E.H. (1912) Second-growth hardwoods in Connecticut, *USDA Forest Service Bulletin*: **96**.

Fusco, F. (2010) Picea+ Tsuga pollen record as a mirror of oxygen isotope signal? An insight into the Italian long pollen series from Pliocene to Early Pleistocene. *Quaternary International*, **225**(1): 58-74

Gates, F. C. (1942) The bogs of northern Lower Michigan. Ecol. Monogr. **12**: 213-254.

Gibson, M.E., McCoy, J., O'Keefe, J.M., Nuñez Otaño, N.B., Warny, S. and Pound, M.J. (2022) Reconstructing terrestrial paleoclimates: a comparison of the Co-existence Approach, Bayesian and probability reconstruction techniques using the UK Neogene. *Paleoceanography and Paleoclimatology*: e2021PA004358.

Hofmann, C.C. and Zetter, R. (2005) Reconstruction of different wetland plant habitats of the Pannonian Basin System (Neogene, Eastern Austria). *Palaios*, **20**(3): 266-279.

Hui, Z., Li, J., Xu, Q., Song, C., Zhang, J., Wu, F. and Zhao, Z. (2011) Miocene vegetation and climatic changes reconstructed from a sporopollen record of the Tianshui Basin, NE Tibetan Plateau. Palaeogeography, Palaeoclimatology, Palaeoecology, **308**(3-4): 373-382.

Hui, Z., Zhang, J., Ma, Z., Li, X., Peng, T., Li, J. and Wang, B. (2018) Global warming and rainfall: Lessons from an analysis of Mid-Miocene climate data. Palaeogeography, palaeoclimatology, palaeoecology, **512**: 106-117.

Hunter, S.J., Haywood, A.M., Valdes, P.J., Francis, J.E., Pound, M.J. (2013) Modelling equable climates of the Late Cretaceous: Can new boundary conditions resolve data–model discrepancies? *Palaeogeography, Palaeoclimatology, Palaeoecology*, **392**: 41-51.

Igarashi, Y., Irino, T., Sawada, K., Song, L. and Furota, S. (2018) Fluctuations in the East Asian monsoon recorded by pollen assemblages in sediments from the Japan Sea off the southwestern coast of Hokkaido, Japan, from 4.3 Ma to the present. Global and planetary change, **163**: 1-9.

IPCC (2022) Climate Change 2022: Impacts, Adaptation, and Vulnerability. Contribution of Working Group II to the Sixth Assessment Report of the Intergovernmental Panel on Climate Change [H.-O. Pörtner, D.C. Roberts, M. Tignor, E.S. Poloczanska, K. Mintenbeck, A. Alegría, M. Craig, S. Langsdorf, S. Löschke, V. Möller, A. Okem, B. Rama (eds.)]. Cambridge University Press. In Press.

Ivanov, D., Ashraf, A.R., Utescher, T., Mosbrugger, V. and Slavomirova, E. (2007a) Late Miocene vegetation and climate of the Balkan region: palynology of the Beli Breg Coal Basin sediments. *Geologica Carpathica*, **58**(4): 367-381.

Ivanov, D., Bozukov, V. and Koleva-Rekalova, E. (2007b) Late Miocene flora from SE Bulgaria: vegetation, landscape and climate reconstruction. Phytologia Balcanica, **13**(3): 281-292.

Jiménez-Moreno, G., Fauquette, S. and Suc, J.P. (2008) Vegetation, climate and palaeoaltitude reconstructions of the Eastern Alps during the Miocene based on pollen records from Austria, Central Europe. Journal of Biogeography, **35**(9): 1638-1649.

Joniak, P., Šujan, M., Fordinál, K., Braucher, R., Rybár, S., Kováčová, M., Kováč, M., Aumaître, G., Bourlès, D.L. and Keddadouche, K. (2020) The age and paleoenvironment of a late Miocene floodplain alongside Lake Pannon: Rodent and mollusk biostratigraphy coupled with authigenic 10Be/9Be dating in the northern Danube Basin of Slovakia. Palaeogeography, Palaeoclimatology, Palaeoecology, **538**: 109482.

Kern, A.K., Harzhauser, M., Soliman, A., Piller, W.E. and Gross, M. (2012) Precipitation driven decadal scale decline and recovery of wetlands of Lake Pannon during the Tortonian, **317**: 1-12.

Kvaçek, Z. (2004) Early Miocene freshwater and swamp ecosystems of the Most Basin (northern Bohemia) with particular reference to the Bílina Mine section. *Journal of Geosciences*, **49**(1-2): 1-40.

Lähteenoja, O., Ruokolainen, K., Schulman, L. and Alvarez, J. (2009) Amazonian floodplains harbour minerotrophic and ombrotrophic peatlands. Catena, **79**(2): 140-145.

Larsson, L.M., Dybkjær, K., Rasmussen, E.S., Piasecki, S., Utescher, T. and Vajda, V. (2011) Miocene climate evolution of northern Europe: A palynological investigation from Denmark. *Palaeogeography, Palaeoclimatology, Palaeoecology*, **309**(3-4): 161-175.

Martinetto, E., Momohara, A., Bizzarri, R., Baldanza, A., Delfino, M., Esu, D. and Sardella, R. (2017) Late persistence and deterministic extinction of “humid thermophilous plant taxa of East Asian affinity”(HUTEA) in southern Europe. *Palaeogeography, Palaeoclimatology, Palaeoecology*, **467**: 211-231.

Micheels, A., Bruch, A.A., Eronen, J., Fortelius, M., Harzhauser, M., Utescher, T. and Mosbrugger, V. (2011) Analysis of heat transport mechanisms from a Late Miocene model experiment with a fully-coupled atmosphere–ocean general circulation model. *Palaeogeography, Palaeoclimatology, Palaeoecology*, **304**(3-4): 337-350.

Micheels, A., Bruch, A.A., Uhl, D., Utescher, T. and Mosbrugger, V. (2007) A Late Miocene climate model simulation with ECHAM4/ML and its quantitative validation with terrestrial proxy data. *Palaeogeography, Palaeoclimatology, Palaeoecology*, **253**(1-2): 251-270.

Montes, C., Cardona, A., Jaramillo, C., Pardo, A., Silva, J.C., Valencia, V., Ayala, C., Pérez-Angel, L.C., Rodriguez-Parra, L.A., Ramirez, V. and Niño, H. (2015) Middle Miocene closure of the Central American seaway. *Science*, **348**(6231): 226-229.

Mosbrugger, V. and Utescher, T. (1997) The coexistence approach—a method for quantitative reconstructions of Tertiary terrestrial palaeoclimate data using plant fossils. *Palaeogeography, Palaeoclimatology, Palaeoecology*, **134**(1-4): 61-86.

Mosbrugger, V., Gee, C.T., Belz, G. and Ashraf, A.R. (1994) Three-dimensional reconstruction of an in-situ Miocene peat forest from the Lower Rhine Embayment, northwestern Germany—new methods in palaeovegetation analysis. *Palaeogeography, Palaeoclimatology, Palaeoecology*, **110**(3-4): 295-317.

Nichols, G.E. (1913) The vegetation of Connecticut II, *Virgin forests, Torreya*, **13**: 199-215.

O''Keefe, J.M., Bechtel, A., Christanis, K., Dai, S., DiMichele, W.A., Eble, C.F., Esterle, J.S., Mastalerz, M., Raymond, A.L., Valentim, B.V. and Wagner, N.J. (2013) On the fundamental difference between coal rank and coal type. International Journal of Coal Geology, **118**: 58-87.

O''Keefe, J.M., Pound, M.J., Riding, J.B. and Vane, C.H. (2020) Cellular preservation and maceral development in lignite and wood from the Brassington Formation (Miocene), Derbyshire, UK. *International Journal of Coal Geology*, **222**: 103452.

Page, S., Wust, R. and Banks, C. (2010) Past and present carbon accumulation and loss in Southeast Asian peatlands. Pages News, **18**(1): 25-26.

Parker, A.J. (1985) Compositional gradients in mesophytic forests of eastern North America. Physical Geography, **6**(3): 247-259.

Piwocki, M. and Ziembińska-Tworzydło, M. (1997) Neogene of the Polish Lowlands-lithostratigraphy and pollen-spore zones. *Geological Quarterly*, **41**(1): 21-40.

561 Popova, S., Utescher, T., GROMYKO, D., BRUCH, A. and Mosbrugger, V. (2012) Palaeoclimate evolution
562 in Siberia and the Russian Far East from the Oligocene to Pliocene–evidence from fruit and seed
563 floras. *Turkish Journal of Earth Sciences*, **21**(2): 315-334.

564 Pound, M.J. and McCoy, J. (2021) Palaeoclimate reconstruction and age assessment of the Miocene
565 flora from the Trwyn y Parc solution pipe complex of Anglesey, Wales, UK. *Palynology*, **45**(4): 697-703.

566 Pound, M.J. and Riding, J.B. (2016) Palaeoenvironment, palaeoclimate and age of the Brassington
567 Formation (Miocene) of Derbyshire, UK. *Journal of the Geological Society*, **173**(2): 306-319.

568 Pound, M.J., Haywood, A.M., Salzmann, U. and Riding, J.B. (2012a) Global vegetation dynamics and
569 latitudinal temperature gradients during the Mid to Late Miocene (15.97–5.33 Ma). *Earth-Science*
570 *Reviews*, **112**(1-2): 1-22.

571 Pound, M.J., Haywood, A.M., Salzmann, U., Riding, J.B., Lunt, D.J. and Hunter, S.J. (2011) A Tortonian
572 (late Miocene, 11.61–7.25 Ma) global vegetation reconstruction. Palaeogeography,
573 Palaeoclimatology, Palaeoecology, **300**(1-4): 29-45.

574 Pound, M.J., O''Keefe, J.M. and Marret, F. (2021) An overview of techniques applied to the extraction
575 of non-pollen palynomorphs, their known taphonomic issues and recommendations to maximize
576 recovery. *Geological Society, London, Special Publications*, **511**(1): 63-76.

577 Pound, M.J., O'Keefe, J.M., Nuñez Otaño, N.B. and Riding, J.B. (2019) Three new Miocene fungal
578 palynomorphs from the Brassington Formation, Derbyshire, UK. *Palynology*, **43**(4): 596-607.

579 Pound, M.J., Riding, J.B., Donders, T.H. and Daskova, J. (2012b) The palynostratigraphy of the
580 Brassington Formation (Upper Miocene) of the southern Pennines, central England. *Palynology*, **36**(1):
581 26-37.

582 Preston, D.P. (1996) Harvesting effects on the hydrology of wet pine flats (Doctoral dissertation,
583 Virginia Tech), Blacksburg, Virginia: 1-126.

584 Prista, G.A., Agostinho, R.J. and Cachão, M.A. (2015) Observing the past to better understand
585 thefuture: a synthesis of the Neogene climate inEurope and its perspectives on present
586 climatechange. *Open Geosciences*, **7**(1): 65-83.

587 Quaijtaal, W., Mertens, K.N. and Louwye, S. (2014) Some new acritarch species from the lower and
588 middle Miocene of the Porcupine Basin, North Atlantic Ocean. *Middle Miocene climate change:*
589 *marine palaeoecology and organic geochemistry in the Porcupine Basin*, **39**: 57.

590 Ravazzi, C., Pini, R., Breda, M., Martinetto, E., Muttoni, G., Chiesa, S., Confortini, F. and Egli, R. (2005)
591 The lacustrine deposits of Fornaci di Ranica (late Early Pleistocene, Italian Pre-Alps): stratigraphy,
592 palaeoenvironment and geological evolution. *Quaternary International*, **131**(1): 35-58.

593 Richardson, C.J. (2003) Pocosins: hydrologically isolated or integrated wetlands on the
594 landscape?. *Wetlands*, **23**(3): 563-576.

595 Riding, J.B. (2021) A guide to preparation protocols in palynology. *Palynology*, **45**(sup1): 1-110.

596 Riding, J.B. and Kyffin-Hughes, J.E. (2006) Further testing of a non-acid palynological preparation
597 procedure. *Palynology*, **30**(1): 69-87.

598 Rius, D., Vannière, B., Galop, D. and Richard, H. (2011) Holocene fire regime changes from multiple-
599 site sedimentary charcoal analyses in the Lourdes basin (Pyrenees, France). Quaternary science
600 reviews, **30**(13-14): 1696-1709.

601 Schaetzl, R.J., Burns, S.F., Johnson, D.L. and Small, T.W. (1988) Tree uprooting: review of impacts on
602 forest ecology. *Vegetatio*, **79**(3): 165-176.

603 Schneider, W. (1992) Floral successions in Miocene swamps and bogs of Central Europe. *Zeitschrift für*
604 *geologische Wissenschaften*, **20**: 555-570.

605 Schneider, W. (1995) Palaeohistological studies on Miocene brown coals of Central
606 Europe. *International Journal of Coal Geology*, **28**(2-4): 229-248.

607 Schwintzer, C.R. (1981) Vegetation and nutrient status of northern Michigan bogs and conifer
608 swamps with a comparison to fens. Canadian Journal of Botany, **59**(5): 842-853.

609 Scotese, C.R. and Wright, N. (2018) PALEOMAP paleodigital elevation models (PaleoDEMS) for the
610 Phanerozoic. PALEOMAP Proj: 1-26. Shannon, C.E. and Weaver, W. (1949) *The mathematical theory*
611 *of communication*. The University of Illinois Press, Urbana: 117.

612 Smith, A. (2013) Digital Geological Map of Great Britain, information notes, 2013, *British Geological*
613 *Survey Open Report,* OR/13/007: 1-50.

614 Smith, A. (2013) Digital Geological Map of Great Britain, information notes, 2013. British Geological
615 Survey Open Report, OR/13/007:54.

616 Steinthorsdottir, M., Coxall, H.K., De Boer, A.M., Huber, M., Barbolini, N., Bradshaw, C.D., Burls, N.J.,
617 Feakins, S.J., Gasson, E., Henderiks, J. and Holbourn, A.E. (2021) The Miocene: The future of the
618 past. *Paleoceanography and Paleoclimatology*, **36**(4): 2020PA004037.

Stuchlik, L., Ziembińska-Tworzydło, M., Kohlman-Adamska, A., Grabowksa, I., Ważyńska, H., Słodkowska, B. and Sadowska, A. (2001) Volume 1 – Spores In Atlas of pollen and spores of the Polish Neogene, W. Szafer Institute of Botany, Polish Academy of Sciences, Kraków, ISBN: 83-85444-79-3: 1-158.

Stuchlik, L., Ziembińska-Tworzydło, M., Kohlman-Adamska, A., Grabowksa, I., Ważyńska, H., and Sadowska, A. (2002) Volume 2- Gymnosperms In Atlas of pollen and spores of the Polish Neogene, W. Szafer Institute of Botany, Polish Academy of Sciences, Kraków, ISBN: 83-85444-92-0: 1-237.

Stuchlik, L., Ziembińska-Tworzydło, M., Kohlman-Adamska, A., Grabowksa, I., Słodkowska, B., Ważyńska, H. and Sadowska, A. (2009) Volume 3 – Angiosperms (1) In Atlas of pollen and spores of the Polish Neogene, W. Szafer Institute of Botany, Polish Academy of Sciences, Kraków, ISBN: 978- 83-89648-74-7:1-235.

Stuchlik, L., Ziembińska-Tworzydło, M., Kohlman-Adamska, A., Grabowksa, I., Słodkowska, B., Worobiec, E., Durska, E. (2014) Volume 4 – Angiosperms (2) In Atlas of pollen and spores of the Polish Neogene, W. Szafer Institute of Botany, Polish Academy of Sciences, Kraków, ISBN: 978-83-62975- 23-5: 1-466.

Super, J.R., Thomas, E., Pagani, M., Huber, M., O''Brien, C.L. and Hull, P.M. (2020) Miocene evolution of North Atlantic Sea surface temperature. *Paleoceanography and Paleoclimatology*, **35**(5): e2019PA003748.

Szulc, J. and Worobiec, E. (2012) Neogene karst sinkhole and its deposits from Górażdże Quarry, Upper Silesia-archive for palaeoenvironmental reconstructions. In *Annales Societatis Geologorum Poloniae*. **82**(4): 371-385.

Thompson, R.S., Anderson, K.H., Bartlein, P.J. (1999) Atlas of relations between climatic parameters and distributions of important trees and shrubs in NorthAmerica. USGS Professional Paper, **650A&B**.

Uemura, K. (1986) A note on Tertiary Sciadopitys (Coniferopsida) from Japan. Bulletin of the National. Science Museum, Tokyo, Series C, **12**: 53-60.

Utescher, T., Ashraf, A.R., Kern, A.K. and Mosbrugger, V. (2021) Diversity patterns in microfloras recovered from Miocene brown coals of the lower Rhine Basin reveal distinct coupling of the structure of the peat-forming vegetation and continental climate variability. *Geological Journal*, **56**(2): 768-785.

Utescher, T., Bondarenko, O.V. and Mosbrugger, V. (2015) The Cenozoic Cooling–continental signals from the Atlantic and Pacific side of Eurasia. *Earth and Planetary Science Letters*, **415**: 121-133.

649 Utescher, T., Bruch, A.A., Erdei, B., François, L., Ivanov, D., Jacques, F.M.B., Kern, A.K., Mosbrugger, V.
650 and Spicer, R.A. (2014) The Coexistence Approach—theoretical background and practical
651 considerations of using plant fossils for climate quantification. *Palaeogeography, Palaeoclimatology,*
652 *Palaeoecology*, **410**: 58-73.

653 Utescher, T., Dreist, A., Henrot, A.J., Hickler, T., Liu, Y.S.C., Mosbrugger, V., Portmann, F.T. and
654 Salzmann, U. (2017) Continental climate gradients in North America and Western Eurasia before and
655 after the closure of the Central American Seaway. *Earth and Planetary Science Letters*, **472**: 120-130.

656 Utescher, T., Erdei, B., Hably, L. and Mosbrugger, V. (2017) Late Miocene vegetation of the
657 Pannonian basin. Palaeogeography, Palaeoclimatology, Palaeoecology, **467**: 131-148.

658 Van Dam, J.A. (2006) Geographic and temporal patterns in the late Neogene (12–3 Ma) aridification
659 of Europe: the use of small mammals as paleoprecipitation proxies. *Palaeogeography,*
660 *Palaeoclimatology, Palaeoecology*, **238**(1-4): 190-218.

661 Velitzelos, D., Bouchal, J.M. and Denk, T. (2014) Review of the Cenozoic floras and vegetation of
662 Greece. Review of Palaeobotany and Palynology, **204**: 56-117.

663 Verb, R.G. and Rubino, D.L. (2012) A Preliminary Survey of Diatom Taxa from Old-Growth Forest Tip-
664 up Pools in Southeastern Indiana Flatwoods. In *Proceedings of the Indiana Academy of Science*, **121**(1):
665 1-7.

666 Walsh, P.T., Atkinson, K., Boulter, M.C. and Shakesby, R.A. (1987) The Oligocene and Miocene outliers
667 of west Cornwall and their bearing on the geomorphological evolution of Oldland
668 Britain. *Philosophical Transactions of the Royal Society of London. Series A, Mathematical and Physical*
669 *Sciences*: 211-245.

670 Walsh, P.T., Banks, V.J., Jones, P.F., Pound, M.J. and Riding, J.B. (2018) A reassessment of the
671 Brassington Formation (Miocene) of Derbyshire, UK and a review of related hypogene karst
672 suffosion22uffusion processes. *Journal of the Geological Society*, **175**(3): 443-463.

673 Walsh, P.T., Boulter, M.C., Ijtaba, M. and Urbani, D.M. (1972) The preservation of the Neogene
674 Brassington Formation of the southern Pennines and its bearing on the evolution of Upland
675 Britain. *Journal of the Geological Society*, **128**(6): 519-559.

676 Walsh, P.T., Collins, P., Ijtaba, M., Newton, J.P., Scott, N.H., Turner, P.R. (1980) Palaeocurrent
677 directions and their bearing on the origin of the Brassington Formation (Miocene-Pliocene) of the
678 southern Pennines, Derbyshire, England, *Mercian Geologist*, **8**(1): 47-61.

679 Wei, X.Z., Jiang, M.X., Huang, H.D., Yang, J.Y. and Yu, J. (2010) Relationships between environment and
680 mountain riparian plant communities associated with two rare tertiary-relict tree species, Euptelea
681 pleiospermum (Eupteleaceae) and Cercidiphyllum japonicum (Cercidiphyllaceae). *Flora-Morphology,*
682 *Distribution, Functional Ecology of Plants*, **205**(12): 841-852.

683 Wilbur, R.L. (1994) The Myricaceae of the United States and Canada: genera, subgenera, and series.
684 SIDA, contributions to botany: 93-107.

685 Wilbur, R.L. (2002) The identity and history of Myrica caroliniensis (Myricaceae). Rhodora: 31-41.

686 Wilde, V. and Riegel, W. (2021) A middle Eocene treefall pit and its filling: a microenvironmental study
687 from the onset of a forest mire in the Geiseltal (Germany). *Palaeobiodiversity and*
688 *Palaeoenvironments*: 1-15.

689 Wolf, M., Lehndorff, E., Wiesenberg, G.L., Stockhausen, M., Schwark, L. and Amelung, W. (2013)
690 Towards reconstruction of past fire regimes from geochemical analysis of charcoal. Organic
691 Geochemistry, **55**: 11-21.

692 Worobiec, E., Widera, M., Worobiec, G. and Kurdziel, B. (2021) Middle Miocene palynoflora from the
693 Adamów lignite deposit, central Poland. *Palynology*, **45**(1): 59-71.

694 Yorke, C. (1954) *The pocket deposits of Derbyshire*. 3 volumes. Privately Published by the author.

695 Yorke, C. (1960) *The Pocket Deposits of Derbyshire: A General Survey*. Privately Published by the
696 Author.

697 You, Y. (2010) Climate-model evaluation of the contribution of sea-surface temperature and carbon
698 dioxide to the Middle Miocene Climate Optimum as a possible analogue of future climate change.
699 Australian Journal of Earth Sciences, **57**(2): 207-219.

700

701

*Table 1: List of pollen microfossils found in previous studies on the Brassington Formation. Names highlighted in bold represent recovered fossilised leaves, * represent recovered seeds. Table is based on findings by Boulter and Chaloner, 1970; Boulter, 1970; Boulter et al., 1971; Boulter, 1974; Pound et al., 2012b; Pound and Riding, 2016; Pound et al., 2019; O'Keefe et al., 2020. Nearest living relatives were assigned using botanical affinities listed by Stuchlik* et al*. (2001; 2002; 2009; 2014).*

Order	Family	Taxa	NLR
Fungi	Chaetosphaeriaceae	*Chaetosphaeria elsikii*	*Chaetosphaeria*
	Incertae sedis	*Rhexocampulliera stogieana*	*Rhexocampulliera*
		R. sufflata	
Bryophyta	Hypnodendraceae	*Hypnodendron sp.*	*Hypnodendron*
		Muscites lanceolata	Unknown
	Sphagnaceae	*Stereisporites crucis*	*Sphagnum*
		S. germanicus rheanus	
		S. granistercoides	
		S. magnoides	
		S. microcornales	
		S. minimoides	
		S. minor microstereis	
		S. pliocenicus pliocenicus	
		S. semigranulus	
		S. stereoides stereoides	
		S. wehningensis	
		S. sp.	
Pteridophyta	Lycopodiaceae	*Lycopodium sp.*	*Lycopodium*
	Gleicheniaceae	*Gleichenidites senonicus*	*Gleichenia*
	Osmundaceae	*Osmunda sp.*	*Osmunda*
	Polypodiaceae	*Laevigatosporites haardtii*	*Polypodium*
		Verrucatosporites favus	
	Polypodiaceae (?)	*Leiotriletes wolffi brevis*	*Lygodium*
		Triplanosporites microsinuosus	*Filicopsida*
	Schizaeaceae (?)	*Leiotriletes wolffi wolffi*	*Lygodium*
	Incertae sedis	*Triplanosporites sinuosus*	*Filicopsida*
Gymnospermae	Cupressaceae	*Cryptomeria anglica*	*Cryptomeria japonica*
		C. sp. *	
		Cupressaceae	Cupressaceae
		Inaperturopollenites hiatus	
		I. dubius	
	Pinaceae	***Abies alba*** *	*Abies*
		Abies sp.	
		Cathaya sp.	*Cathaya*
		Cedrus sp.	*Cedrus*
		Keteleeria sp.	*Keteleeria*
		Picea sp. *	*Picea*
		Pinus sylvestris - type *	*Pinus*
		P. haploxylon - type	
		P. sp.	
		Tsuga canadensis - type	*Tsuga*
		T. diversifolia - type	
		T. sp.	
	Podocarpaceae	*Podocapoidites libellus*	*Podocarpus*
		Podocapus-type	
	Sciadopityaceae	*Sciadopitys sp.*	*Sciadopitys*
		Sciadopitys tertiaria	
Angiospermae	Actinidiaceae	*Actinidia sp.*	*Actinidia*
	Aquifoliaceae	*Ilex sp.*	*Ilex*
		Tricolporopollenites illacus	
		T. margaritas	Aquifoliaceae
	Araliaceae	*Hedera sp.*	*Hedera*

Order	Family	Taxa	NLR
		Tricolpopollenites edmundi	Anacardiaceae
	Brassicaceae?*	*Parrya sp.*	*Parrya*
	Compositae	Compositae	Compositae
		Compositoipollenites ricophorus	*Compositae*
	Betulaceae	*Alnus sp.*	*Alnus*
		Carpinus sp.	*Carpinus*
		Corylus sp.	*Corylus*
		Trivestibulopollenites betuloides	*Betula*
	Caryophyllaceae	Caryophyllaceae	Caryophyllaceae
	Cyrillaceae	*cf. Cyrilla thompsoni*	*Cyrillaceae/Clethraceae*
	Ericaceae	*Calluna sp.*	*Calluna*
		Empetrum sp.	*Empetrum*
		Erica sp.	Ericaceae
		Ericaceae	
		Ericipites baculatus	
		E. callidus	
		E. costatus	
		E. ericius	
		Rhododendron sp.	*Rhododendron*
	Fabaceae?	*Tricolpopollenites ipilensis*	Unknown
		T. lihaiensis fallax	Fabaceae
		T. lihiarensis lihiarensis	
	Fagaceae?	*Quercoidites microhenrici*	Quercus
		Tricolpopollenites microhenrici	
	Hamamelidaceae	*Corylopsis sp.*	*Corylopsis*
		Liquidambar sp.	*Liquidambar*
	Incertae sedis	*Tricolpopollenites sp.*	Unknown
	Juglandaceae	*Carya sp.*	*Carya*
		Juglans sp.	*Juglans*
	Liliaceae	*Smilax sp.*	*Smilax*
	Myricaceae	*Myrica sp.*	*Myrica*
	Nyssaceae	*Nyssa sp.*	*Nyssa*
	Onagraceae	*Corsinipollenites maii*	Onagraceae
	Pentaphylacaceae	*Eurya sp.*	*Eurya*
	Plumbaginaceae	*Armeria sp.*	Plumbaginaceae
		Limonium sp.	*Limonium*
	Poaceae	*Graminidites media*	Poaceae
	Polemoniaceae	*Polemonium sp.*	*Polemonium*
	Polygonaceae	*Polygonum sp.*	*Polygonum*
	Rhamnaceae	*cf. Rhamnus sp.*	*Rhamnus*
	Rubiaceae	*cf. Rubiaceae*	Rubiaceae
	Salicaceae	*Salix sp.*	*Salix*
		Tricolpopollenites retiformis	
	Sapindaceae	*Aesculus sp.*	*Aesculus*
	Sapotaceae	*Tetracolporopollenites sapotoides*	Sapotaceae
	Saxifragaceae	*Saxifraga sp.*	*Saxifraga*
	Smilacaceae	*Periporopollenites echinatus*	*Liquidambar*
	Symplocaceae	*Symplocoipollenites rotundus*	*Symplocos*
		S. vestibulum	
	Trapaceae	*cf. Trapa sp.*	*Trapa*
	Ulmaceae	*Ulmus sp.*	*Ulmus*
		Indeterminate	Unknown

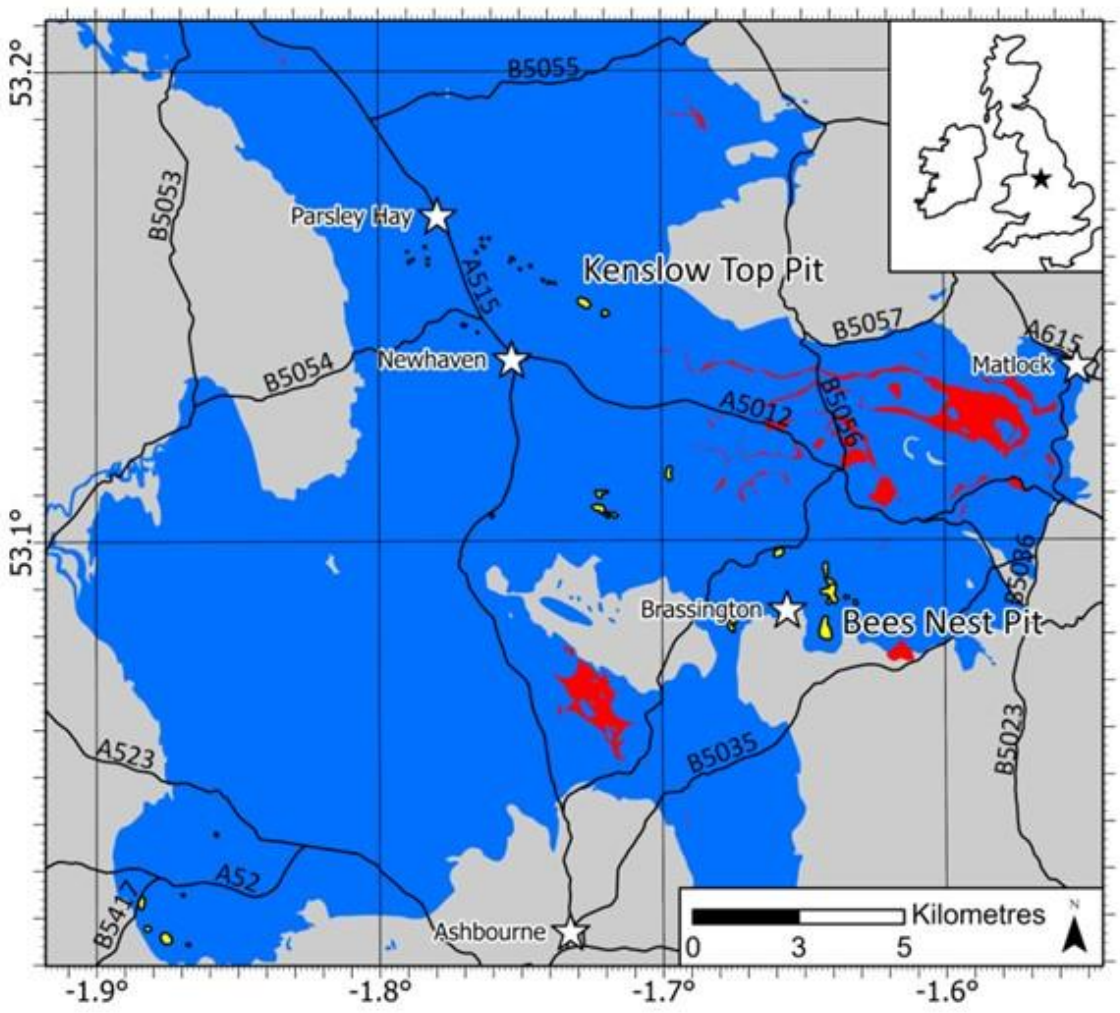

Figure 1 – A simplified geological map of the area where the ~60 known outcrops of the Brassington Formation are located, with an inset map at the top right to illustrate the location of this area in the British Isles. The Brassington Formation is shown in yellow, although most karstic hollows are too small to be visible at this scale and some are visible only as irregular black dots. The Peak Limestone Group (Mississippian/Lower Carboniferous) is shown in blue ornament; the 'pockets' of Brassington Formation are in karstic cavities within this major carbonate unit. The red ornament indicates igneous rocks, dominantly basalt, within the Peak Limestone Group. The grey colour represents several major Pennsylvanian/Upper Carboniferous and Triassic siliciclastic lithostratigraphical units which overlie the Peak Limestone Group in this part of the East Midlands of England. Major roads in the area are included for orientation, together with selected settlements (white stars). The map was generated using ArcGIS Pro. This simplified geological map is based upon the British Geological Survey 1:10000 scale digital geological map (Smith, 2013), using the EDINA Geology Digimap Service. The road network is from the Ordnance Survey Open Roads (SHAPE geospatial data), scale 1:25000, updated on 23 September 2021. Downloaded on 2022-04-13 09:54:41.238. [1.5-column fitting image].

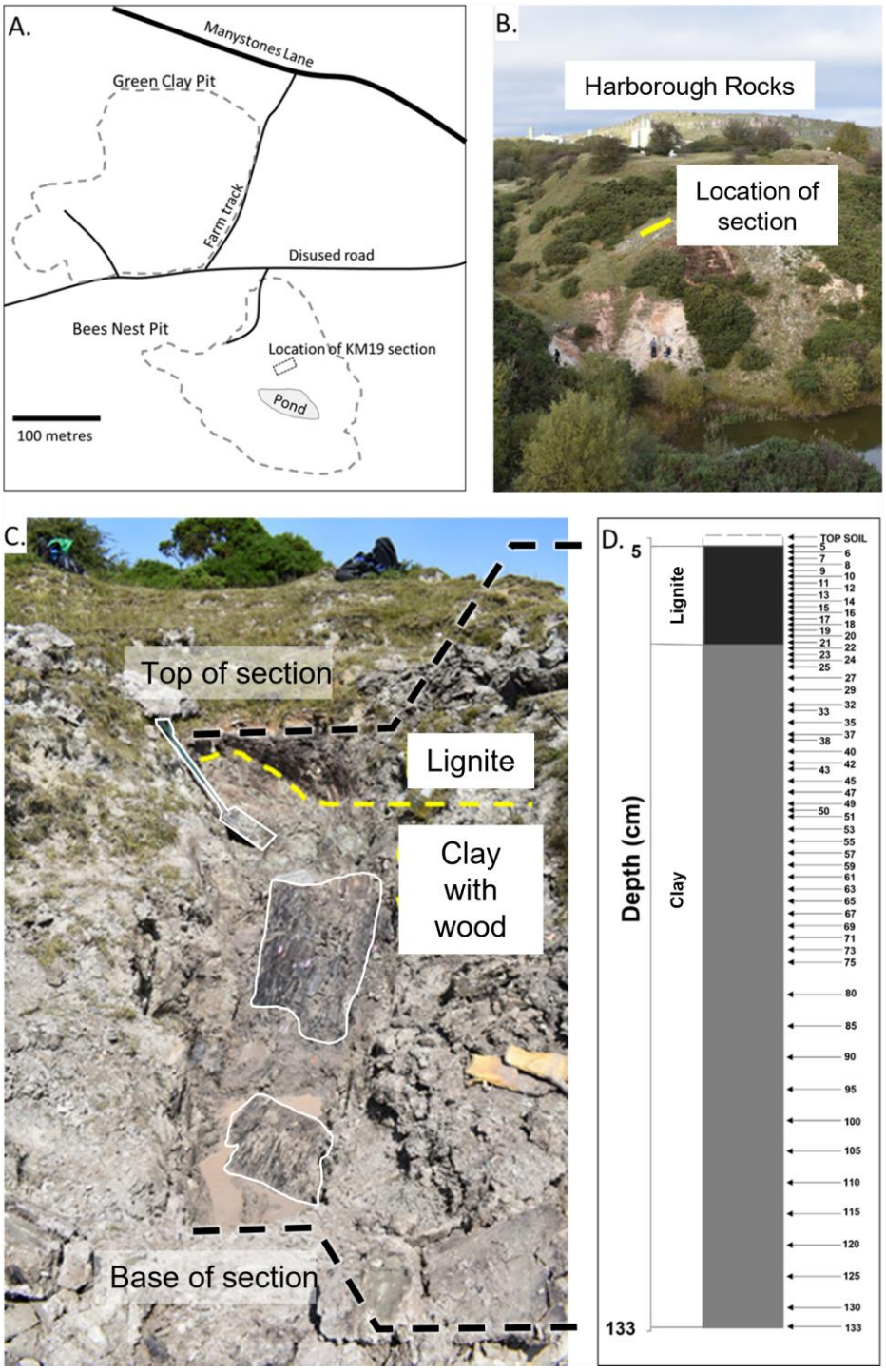
A.
Manystones Lane
Green Clay Pit
Farm track
Disused road
Bees Nest Pit
Location of KM19 section
Pond
100 metres
B.
Harborough Rocks
Location of section
C.
Top of section
Lignite
Clay with wood
Base of section
D.
5
Lignite
Clay
Depth (cm)
133
TOP SOIL

Figure 2 – Location of the KM19 section within the Kenslow Member of the Brassington Formation at Bees Nest Pit. A. Field map of the site showing the location of Bees Nest Pit in relation to Manystones Lane, the nearest access road, and the location of the KM19 section to the north of the pond. B. Field photograph of Bees Nest Pit with the location of the KM19 section highlighted and the location of Harborough Rocks on the north side of Manystones Lane indicated. C. Photograph of the KM19 section with annotated lithology and large fragment of fossil wood in centre of the section (note the spade for scale). D. Lithological log of the KM19 section with palynology samples indicated by arrows; the sample numbers indicate the depth in centimetres. [2-column fitting image].

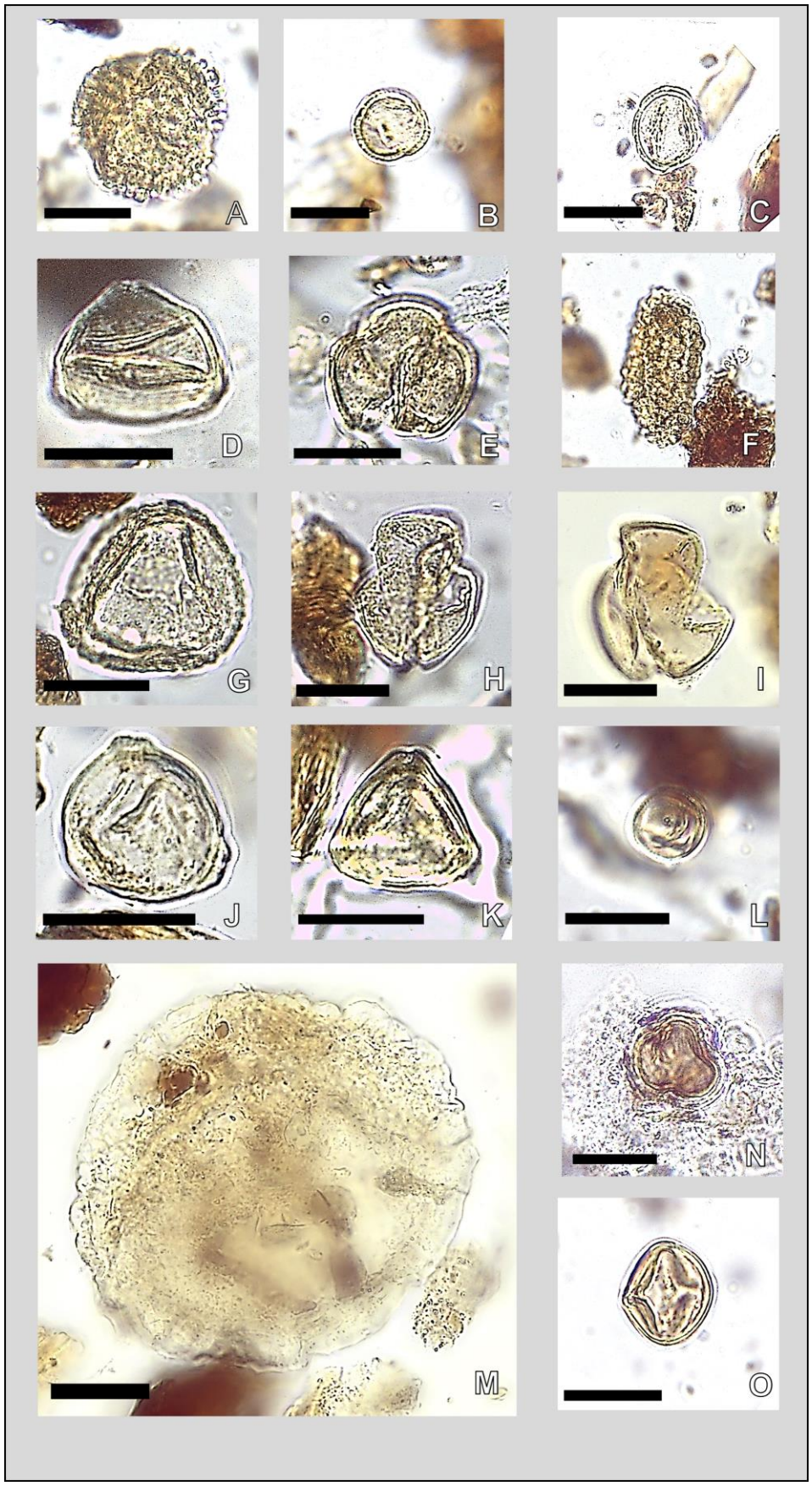
A
B
C
D
E
F
G
H
I
J
K
L
M
N
O


P
Q
R
S
T
U
V
W
X
Y
Z
AA
AB
AC
AD

852

853 *Figure 3: Plates 1-2. Key pollen grains from the Kenslow Member at the Serravallian Bees Nest Pit. 3-*
854 *D, 3-L, 3-O, 3-P, 3-R, 3-S and 3-X were taken from KM19-6, depth 6 cm. 3-B was taken from KM19-8,*
855 *depth 8 cm. 3-N was taken from KM19-130, depth 130 cm. Scale bar on all scaled photographs*
856 *measures 20 µm. Plate 1. 3-A: Ilex-type. 3-B and 3-C: Olea-type. 3-D: Corylus-type. 3-E: Nyssa-type. 3-*
857 *F and 3-G: Sciadopitys-type. 3-H and 3-I: Cercidiphyllum-type. 3-J and 3-K: Betula-type. 3-L: Urtica-*
858 *type. 3-M: Tsuga-type. 3-N: Caprifoliaceae. 3-O: Cyrillaceae/ Clethraceae. Plate 2. 3-P: Salix-type. 3-*
859 *Q: Castaneioideae. 3-R: Tricolpopollenites ipilensis. 3-S: Ericaceae. 3-T: Symplocos-type. 3-U:*
860 *Cyperaceae. 3-V: Myrica-type. 3-W: Quercus-type. 3-X: Platycarya-type. 3-Y, 3-Z and 3-AA:*
861 *Cupressaceae. 3-AB: Abies-type. 3-AC: Pinus-type. 3-AD: Cathaya-type.*

862 . [2-column fitting image]

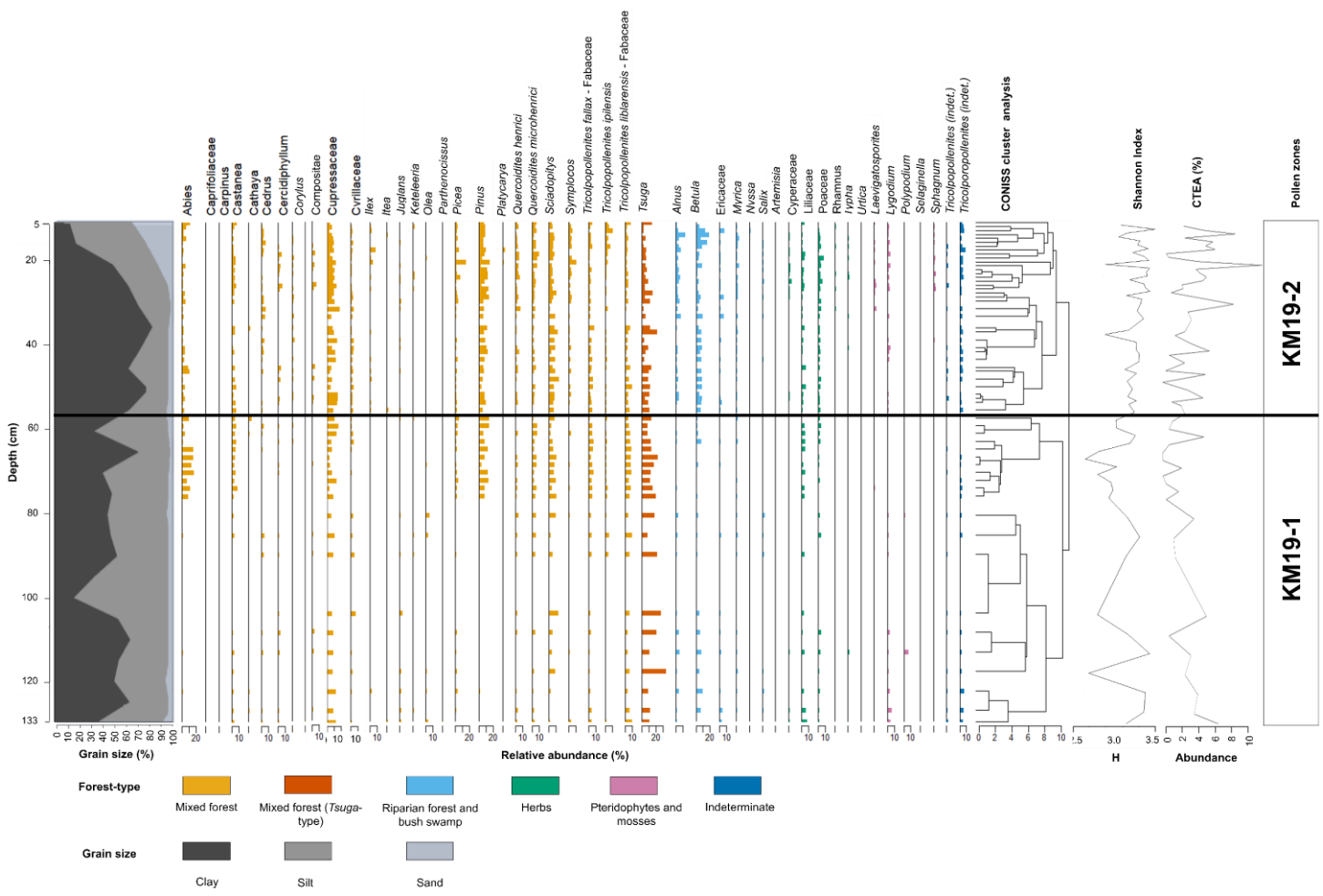
Depth (cm)
Grain size (%)
Relative abundance (%)
Abies
Caprifoliaceae
Carpinus
Castanea
Cathaya
Cedrus
Cercidiphyllum
Corylus
Compositae
Cupressaceae
Cyrillaceae
Ilex
Itea
Juglans
Keteleeria
Olea
Parthenocissus
Picea
Pinus
Platycarya
Quercoidites henrici
Quercoidites microhenrici
Sciadopitys
Symplocos
Tricolpopollenites fallax - Fabaceae
Tricolpopollenites ipilensis
Tricolpopollenites liblarensis - Fabaceae
Tsuga
Alnus
Betula
Ericaceae
Myrica
Nyssa
Salix
Artemisia
Cyperaceae
Liliaceae
Poaceae
Rhamnus
Typha
Urtica
Laevigatosporites
Lygodium
Polypodium
Solaginella
Sphagnum
Tricolpopollenites (indet.)
Tricoloporopollenites (indet.)
CONISS cluster analysis
Shannon index
CTEA (%)
Pollen zones
KM19-2
KM19-1
H
Abundance
Forest-type
Mixed forest
Mixed forest (Tsuga-type)
Riparian forest and bush swamp
Herbs
Pteridophytes and mosses
Indeterminate
Grain size
Clay
Silt
Sand

866 *Figure 4 - Stratigraphical distribution of pollen and spores in the 58 samples of the KM19 section of the Kenslow Member from Bees Nest Pit. Pollen zones*
867 *(KM19-1 and KM19-2) are defined by CONISS. The Shannon Index and CTEA (%) of each depth were calculated and plotted. Colour scheme designed to*
868 *accommodate for colour-blindness. Ecological groupings are based upon Schneider (1992) and Szulc and Worobiec (2012). Sedimentology shows the grain*
869 *size as measured by Mastersizer analysis.* [2-column fitting image]

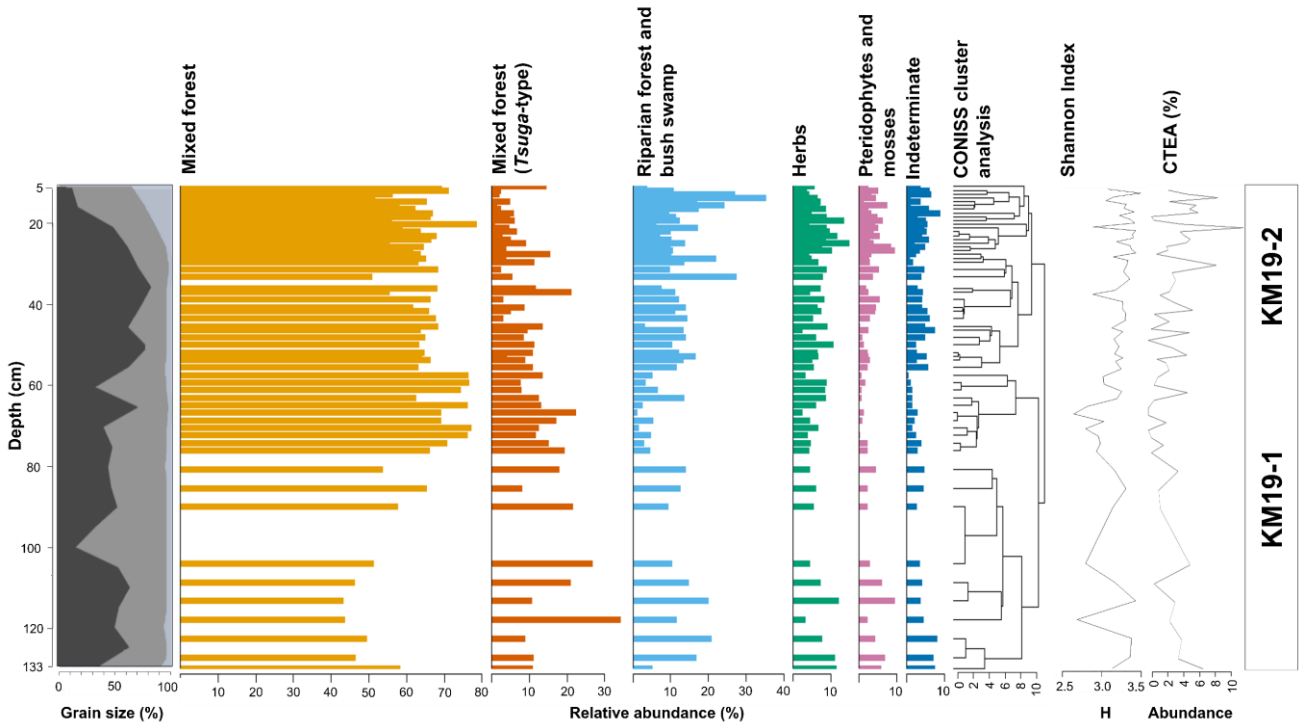

Figure 5 - Summary pollen diagram showing ecological groupings and Tsuga (dominant pollen type), with Shannon Index and relative abundance of CTEA. Colour scheme designed to accommodate for colour-blindness. Pollen zones are the same as Figure 4. [1.5-column fitting image]

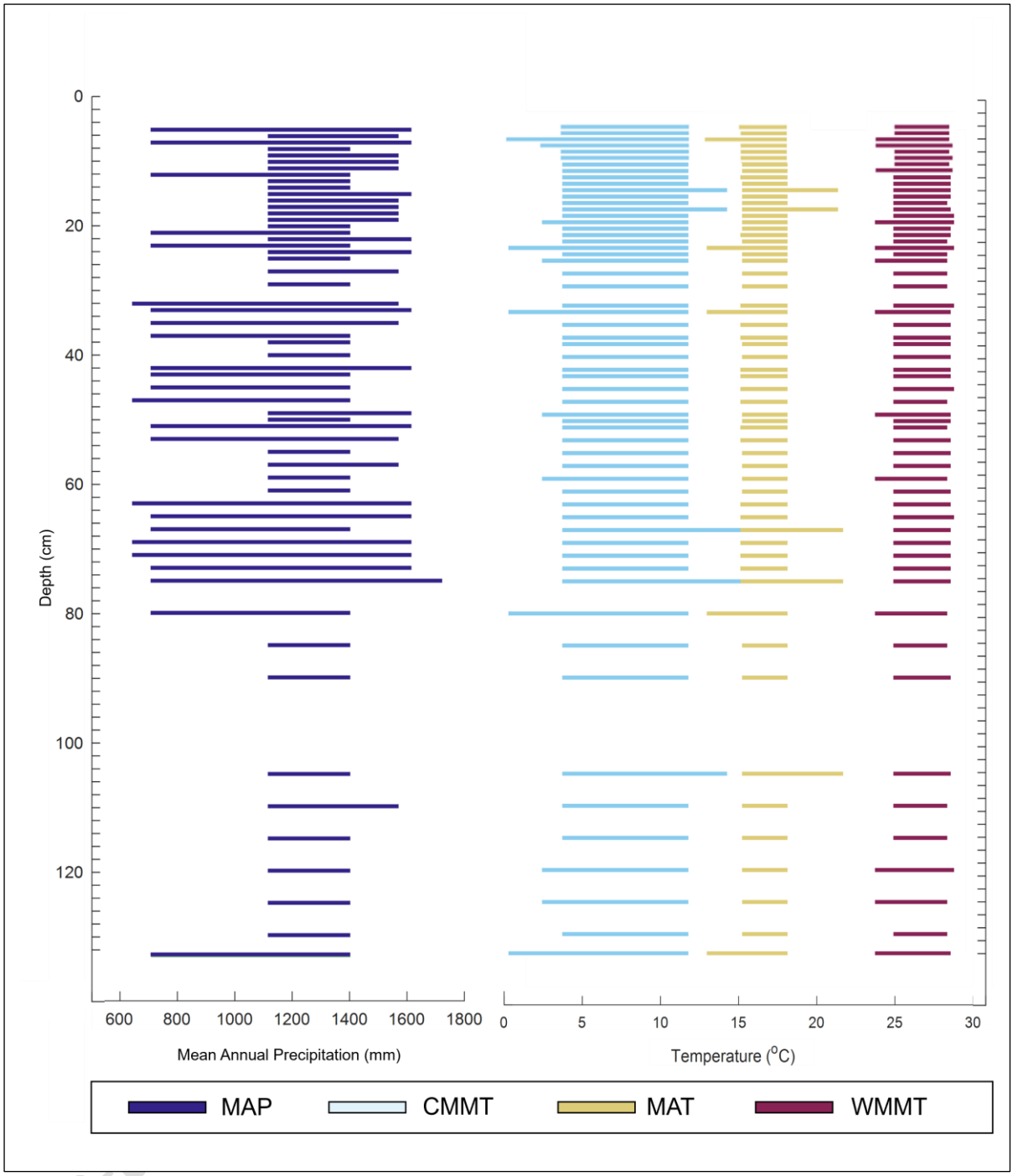

Figure 6 – Temperature and precipitation estimates through the KM19 section of the Kenslow Member, reconstructed using the co-existence approach. [1.5-column fitting image]

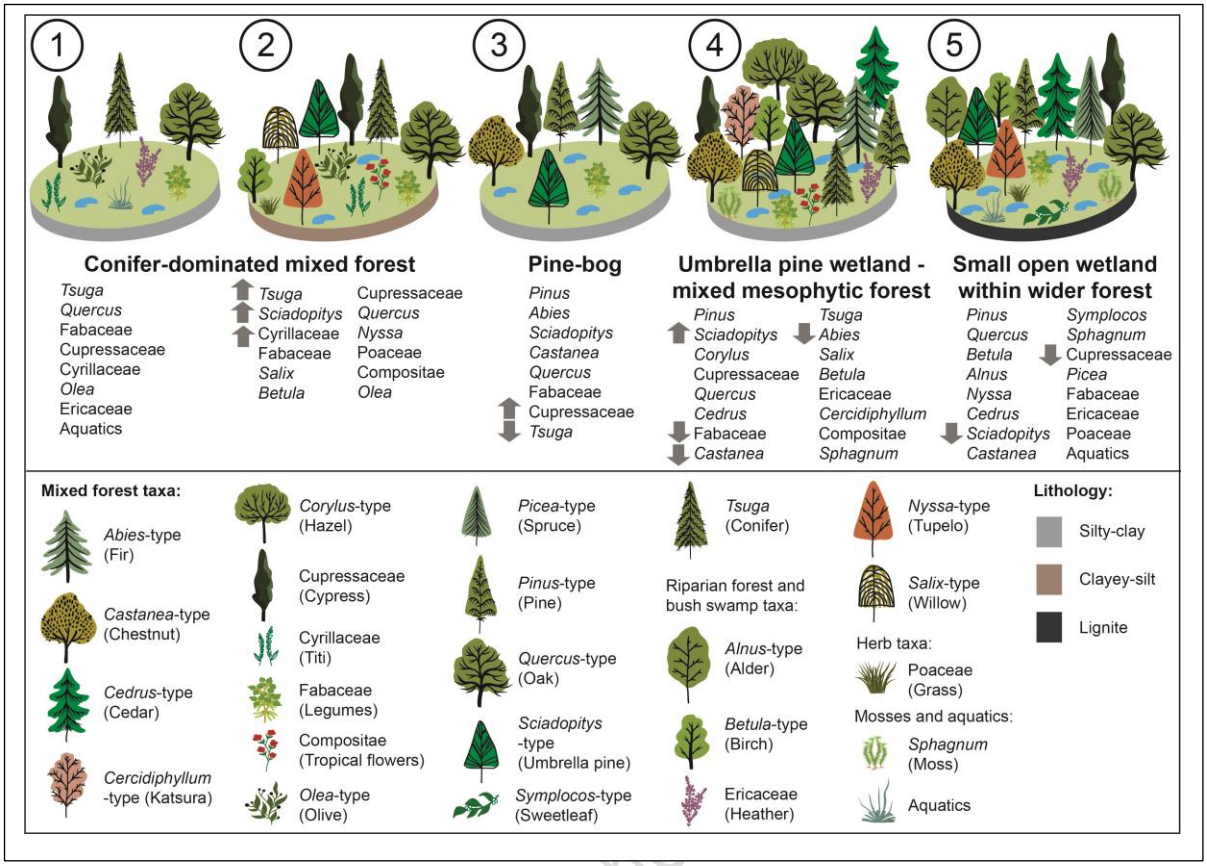

Figure 7 – The main vegetation and sediment grain size changes observed throughout pollen zones KM19-1 (A-C) and KM19-2 (C-E), shown in Figures 4-5. The transition zone between pollen zones is apparent in C; E represents the lignite exclusively. From base to top: stages A-C represent a conifer-dominated mixed forest; stage C reconstructs a pine-dominated bog, stage D represents an umbrella pine wetland and with mixed mesophytic forest elements, and stage E shows the reconstruction of a small open wetland within a wider forest palaeoenvironment. Increases and decreases in relative abundances are indicated by grey arrows. Key taxa are grouped into four main groups, including: mixed forest taxa; riparian forest and bush swamp taxa; herb taxa, and mosses and aquatics. [2-column fitting image]

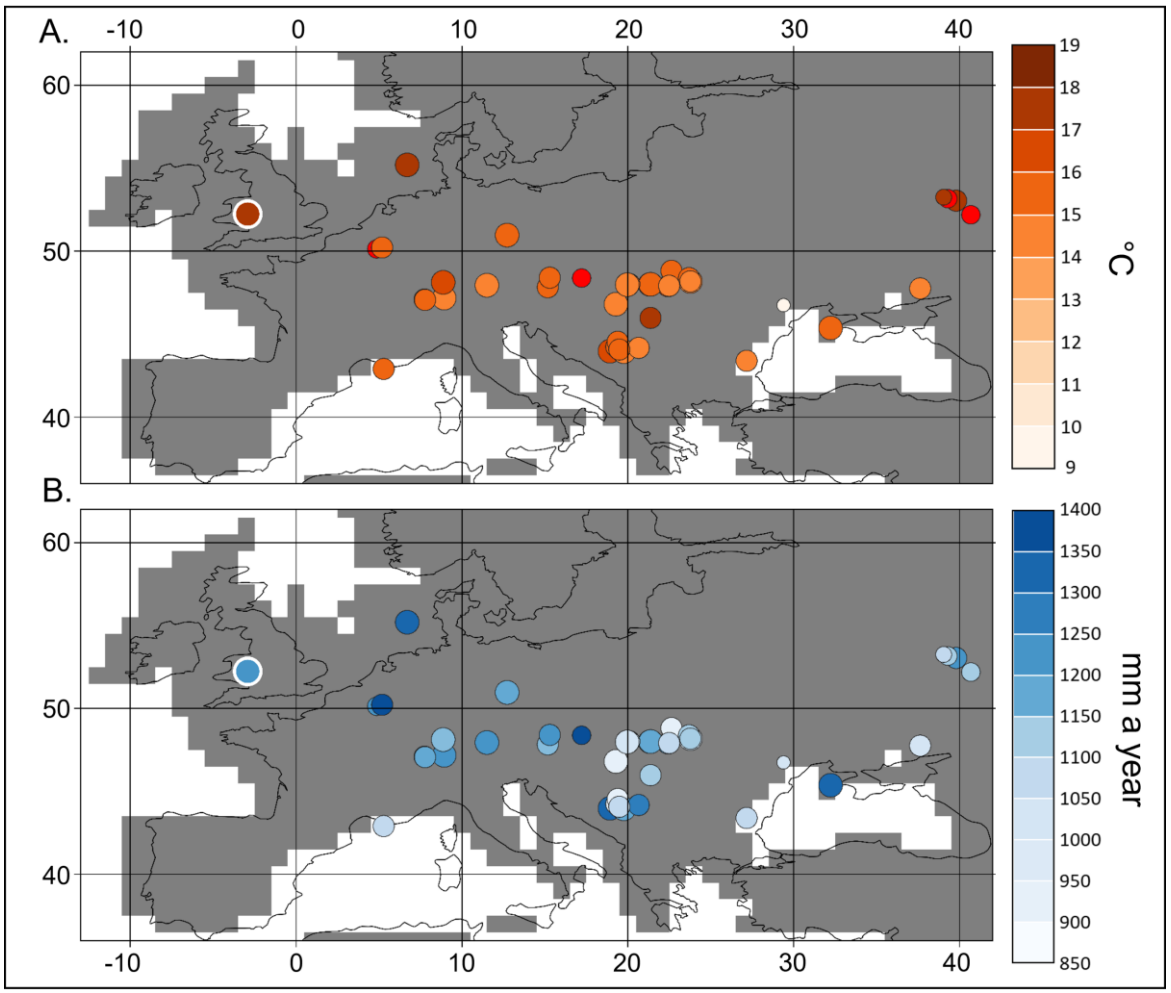

Figure 8 - Palaeogeographical maps of co-existence approach-derived palaeoclimate values across Europe for the Serravallian (Middle Miocene). A = Mean Annual Temperature and B = Mean Annual Precipitation. Because the co-existence approach reconstructs a range, the colour of the dot corresponds to the mid-point of the range, and the size of the dot indicates the range size (bigger dots = smaller ranges). The new Kenslow Member values are shown by the circle with a white outline. The base map palaeogeography is representative of the Middle Miocene (Scotese and Wright 2018), and has the modern coastline superimposed for reader orientation. The modern latitude and longitude follows that of Hunter et al. (2013). List of localities highlighted by circles in the above figure is part of a dataset which is currently in review, as part of another paper. See section Pound, M.J. (2022) in Data Availability for study site coordinates and MAP and MAT ranges of each locality. [1.5-column fitting image]

Supplementary Data

Supplementary Table 1: List of taxa identified during this study with their relative abundance (%) at each surveyed depth – see Figure 2D.

Supplementary Table 2: Co-existence-approach-based results at each surveyed depth. The determinant taxa for palaeoclimate variables MAT, WMMT, CMMT and MAP are shown to the right of values. Taxa highlighted in yellow were present in the palynostratigraphy record with a relative abundance below 1.0%.